Perspectives for the next generation of MeV-GeV gamma-ray space missions

M. Nicola Mazziotta
INFN Bari
mazziotta@ba.infn.it
Advances in Space AstroParticle Physics (ASAPP)
Perugia June 19 – 23, 2023

The Fermi Gamma-ray Space Telescope

- Launched on June 11, 2008
  - June 11, 2023: Happy 15-year birthday, GLAST/Fermi!
- Two instruments:
  - Large Area Telescope (LAT)
  - Gamma Burst Monitor (GBM)
- Mission design lifetime was for a minimum of 5 years, with a goal of 10 years
- Mission extensions through a competitive NASA Senior Review (SR) process
  - 2022 SR
    - Confirmed funds through 2025
    - Invite Fermi at next SR
- Spacecraft status
  - Normal operations, no current areas of concern
- Excellent recognition of Fermi in Astro 2020 Decadal Survey

Science with the Fermi LAT

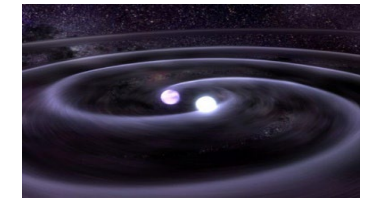

Gravitational waves

Extragalactic

Dark Matter searches

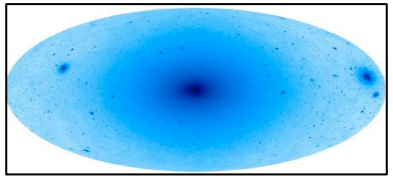

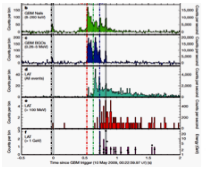

GRBs

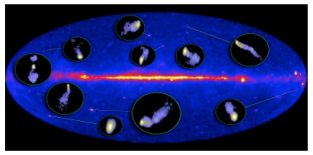

Blazars

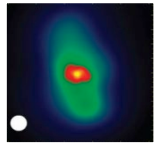

Radio Galaxies

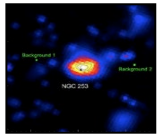

Starburst Galaxies

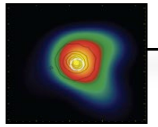

Globular Clusters

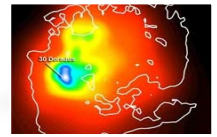

LMC & SMC

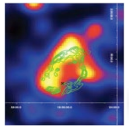

SNRs & PWN

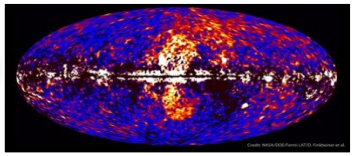

Fermi Bubbles

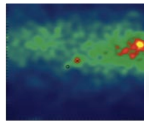

Novae

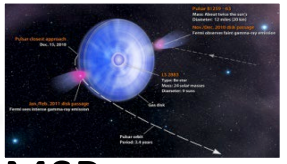

γ-ray Binaries

Pulsars: isolated, binaries, & MSPs

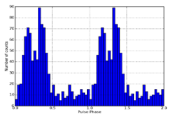

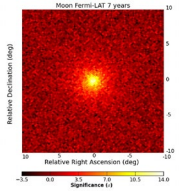

Moon

Earth Limb

Galactic

Sun: flares & CR interactions

Local

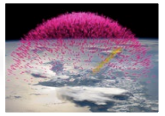

Terrestrial γ-ray Flashes

Unidentified Sources

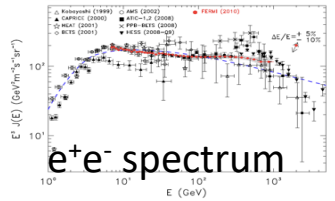

e^+e^- spectrum

Gamma-ray telescope satellite

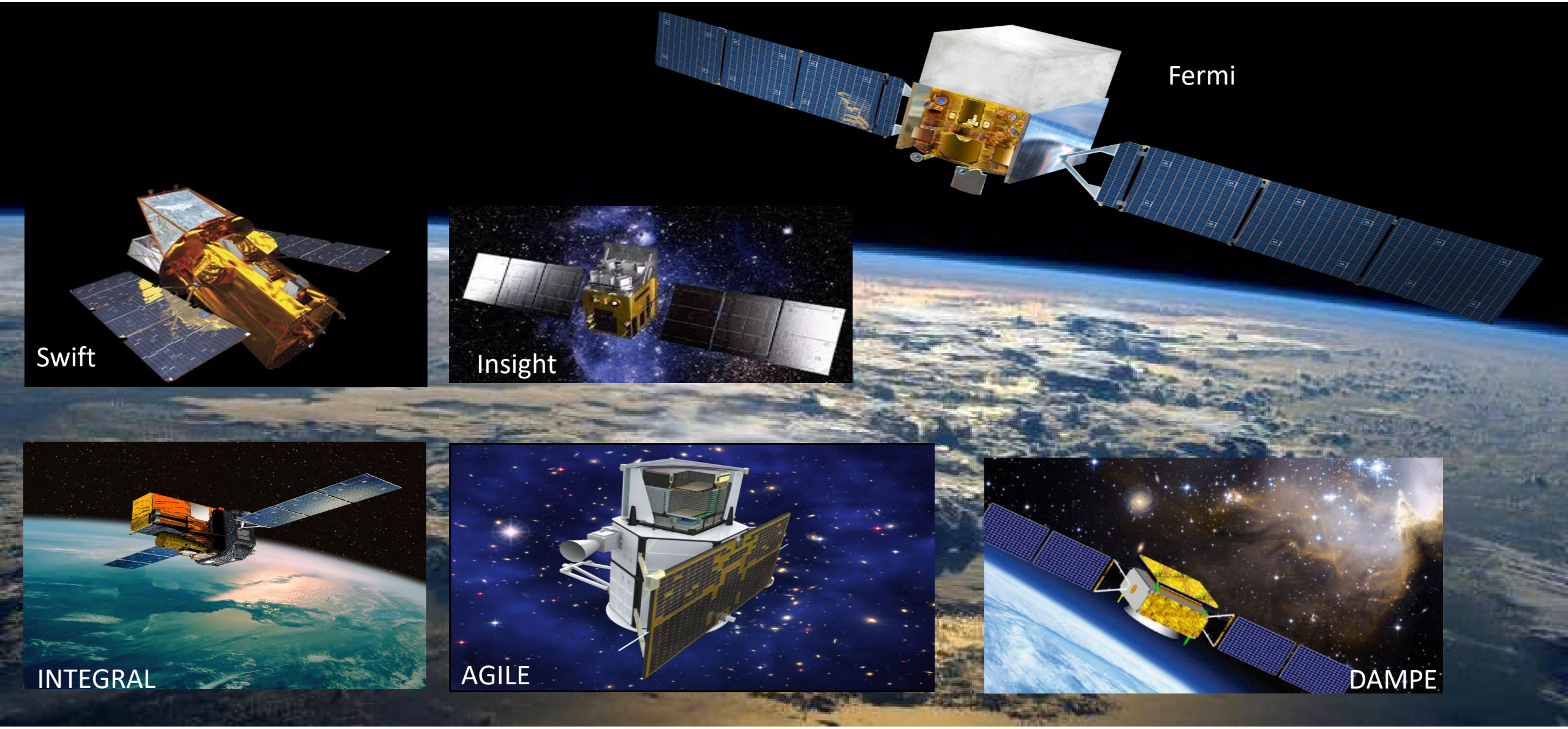

Next generation gamma-ray MeV-GeV experiments

- Poorly covered region of the electromagnetic spectrum (“M”-gap)
  - Only a few tens of steady sources detected so far between 0.2 and 30 MeV
  - Many objects have their peak emissivity in this range (GRBs, blazars, pulsars...)
- New generation of MeV-GeV gamma-ray telescopes
  - Should operate in both Compton and pair conversion regimes
- Need for a sensitive, wide field of view gamma-ray space observatory operating at the same time as facilities like SKA and CTA, as well as GW and neutrino detectors, to get a coherent picture of the transient gamma-ray sky and of the sources of gravitational waves and high-energy neutrinos

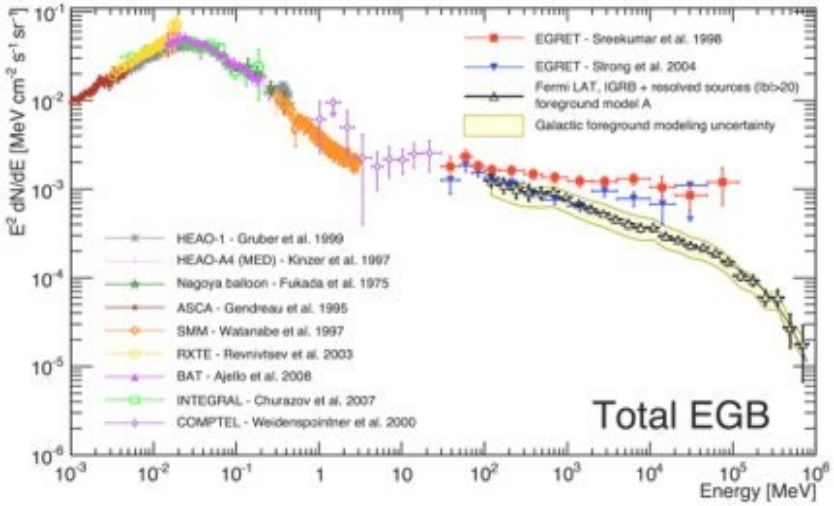

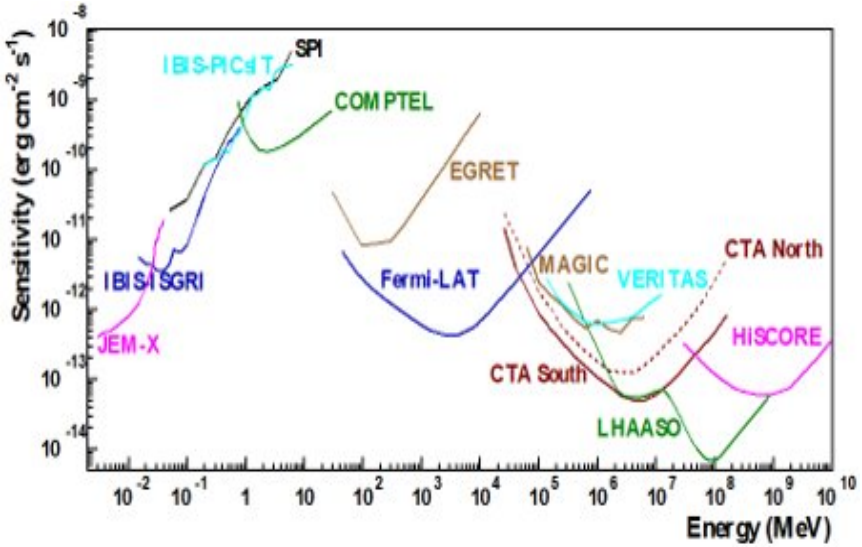

Science motivations (selection)

- Processes at the heart of the extreme Universe (AGNs, GRBs, microquasars): prospects for the Astronomy of the 2030s
- Multi-wavelength, multi-messenger coverage of the sky (with Ligo/Virgo, CTA, SKA, eLISA, ...), with special focus on transient phenomena
- The origin of high-energy particles and impact on galaxy evolution, from cosmic rays to antimatter
- Nucleosynthesis and chemical enrichment of our Galaxy

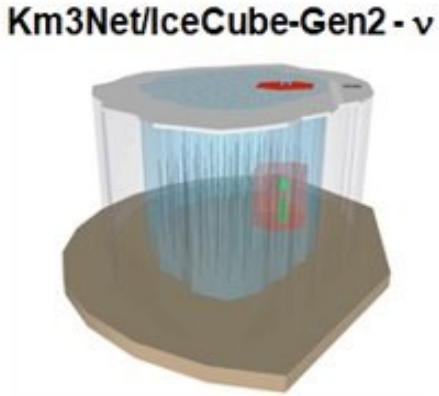

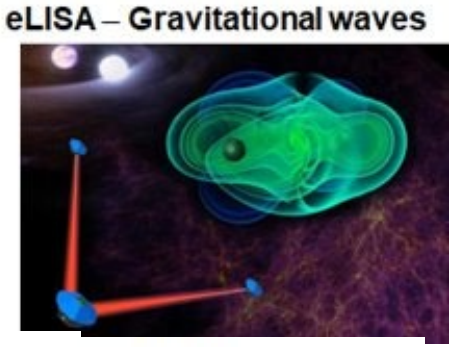

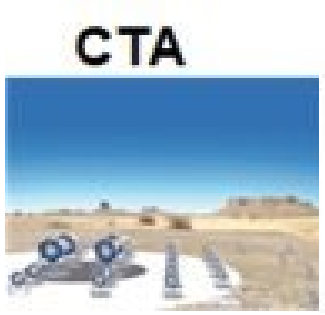

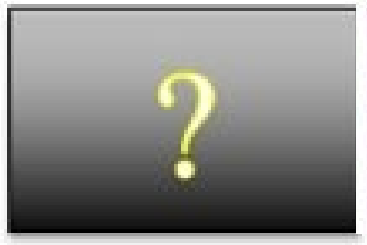

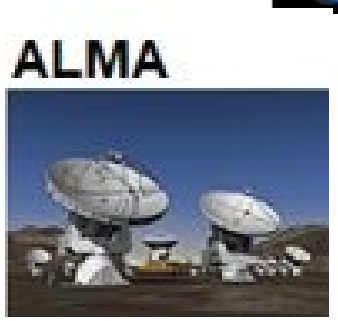

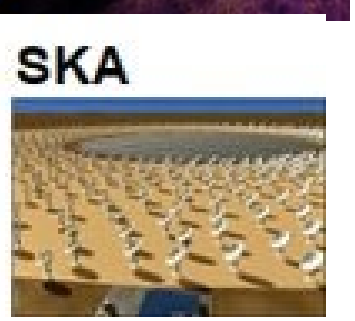

Low/High energy gamma-ray (MeV-GeV) detection in space

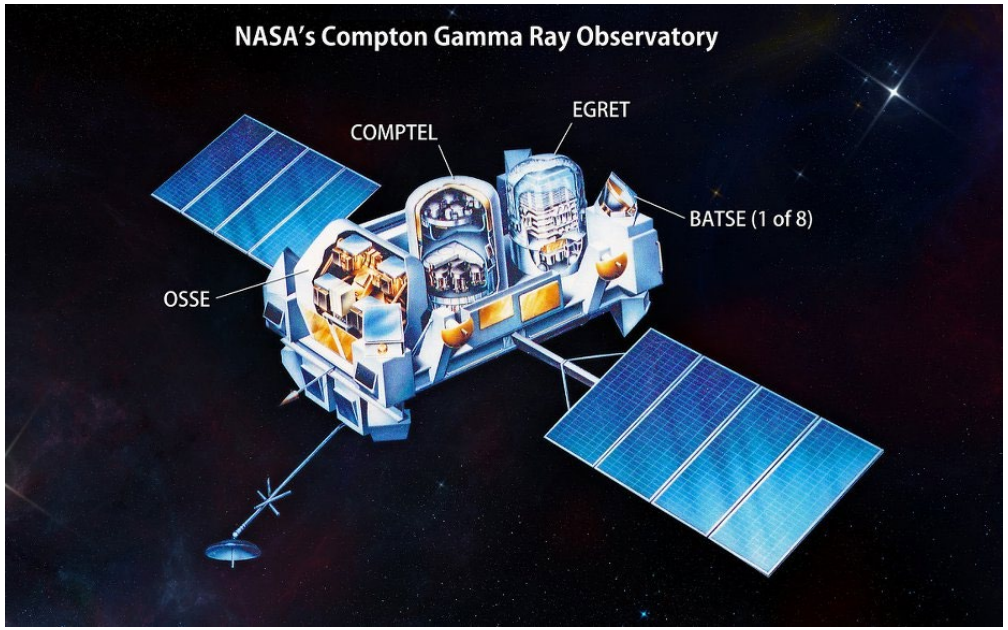

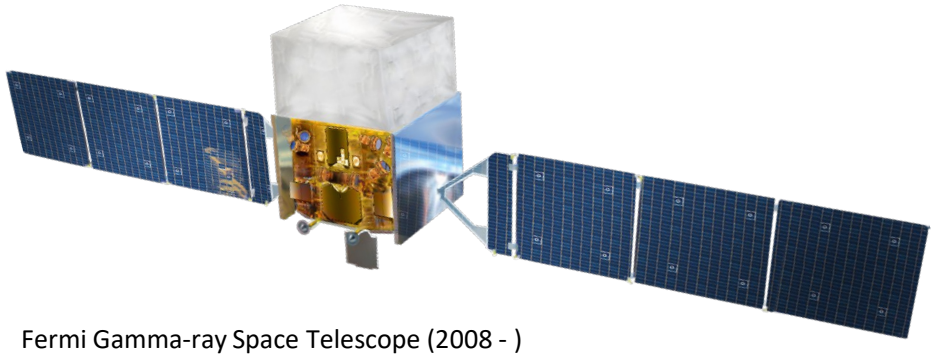

Fermi Gamma-ray Space Telescope (2008 -)
Large Area Telescope (LAT)
Gamma-ray Burst Monitor (GBM)

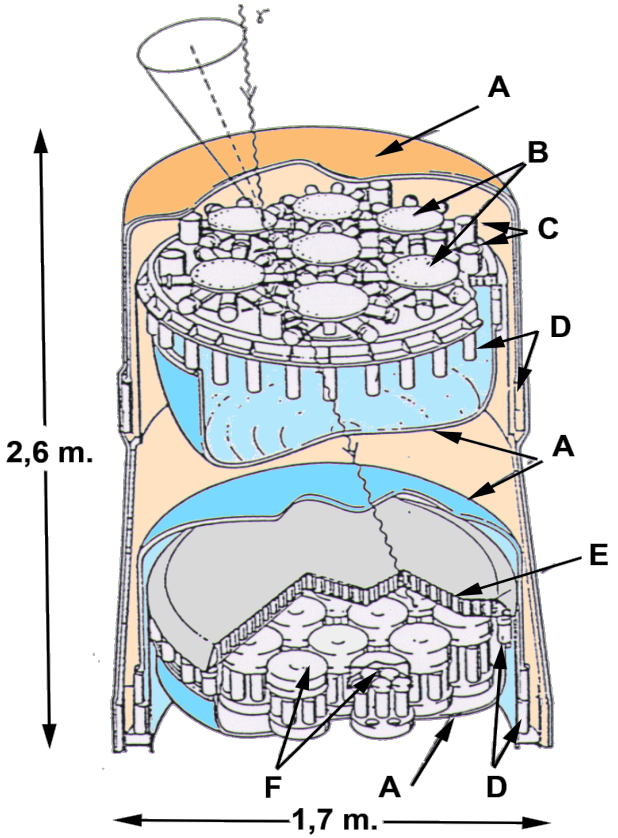

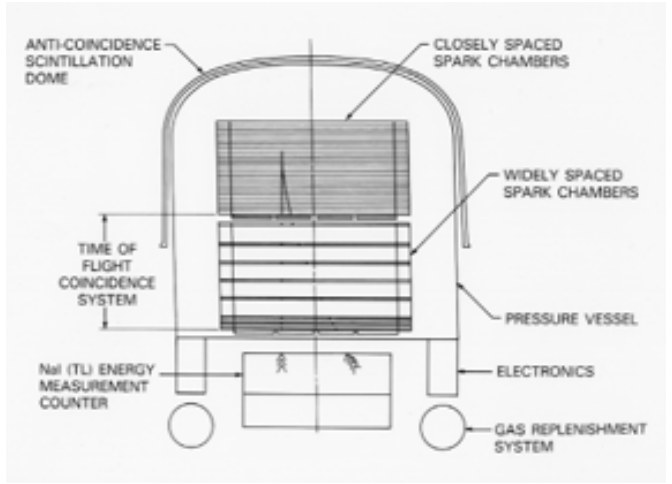

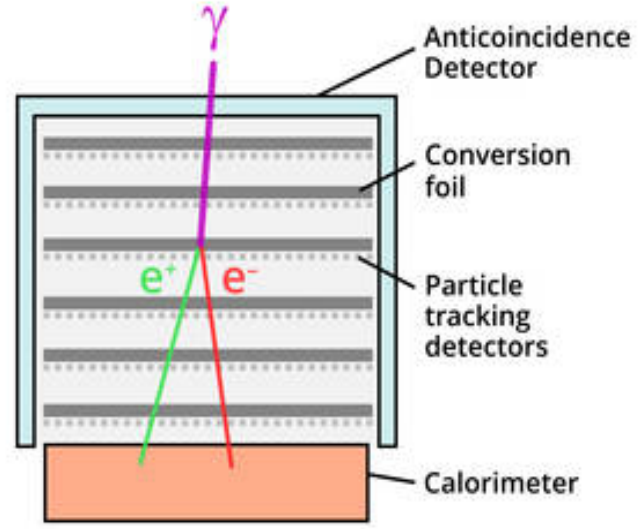

Gamma-ray interactions with matter

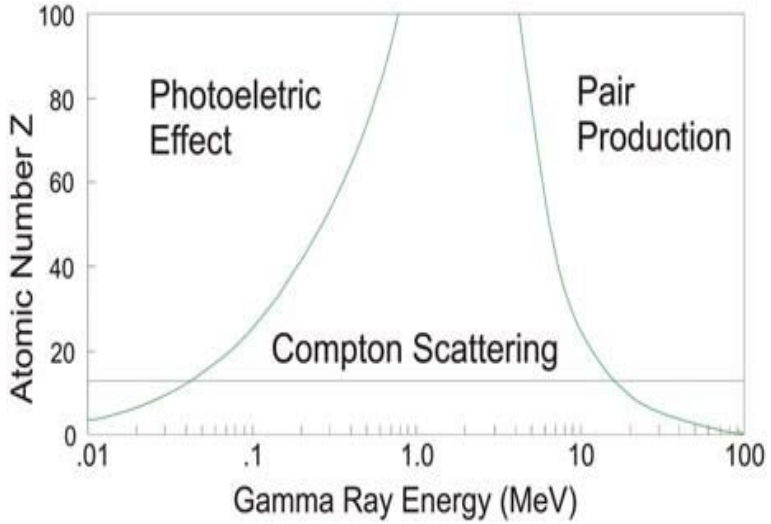

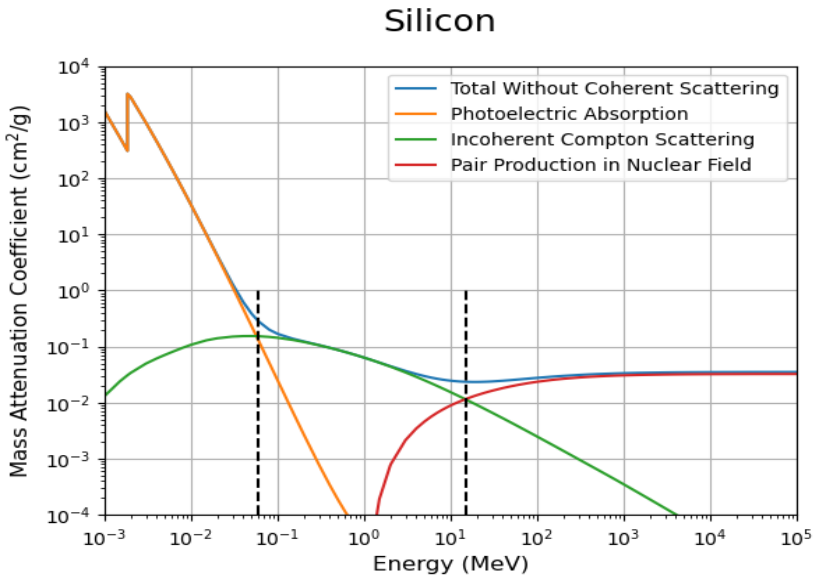

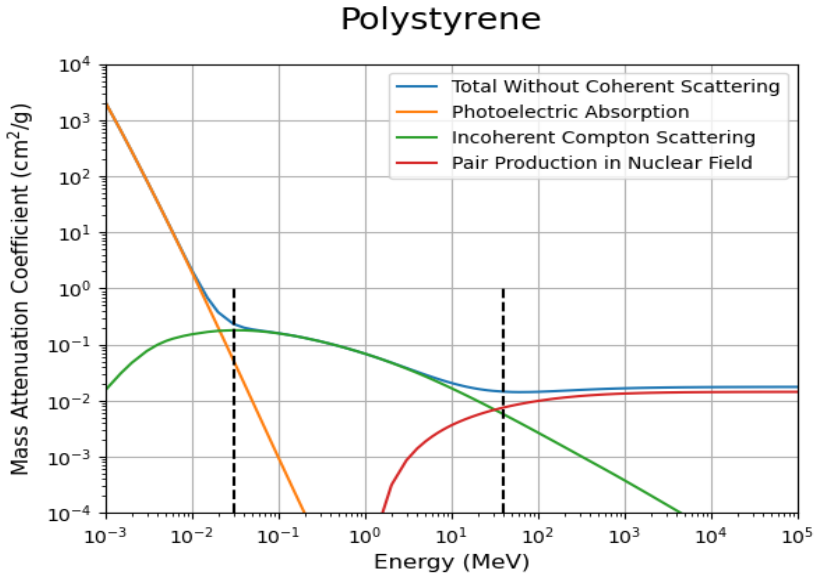

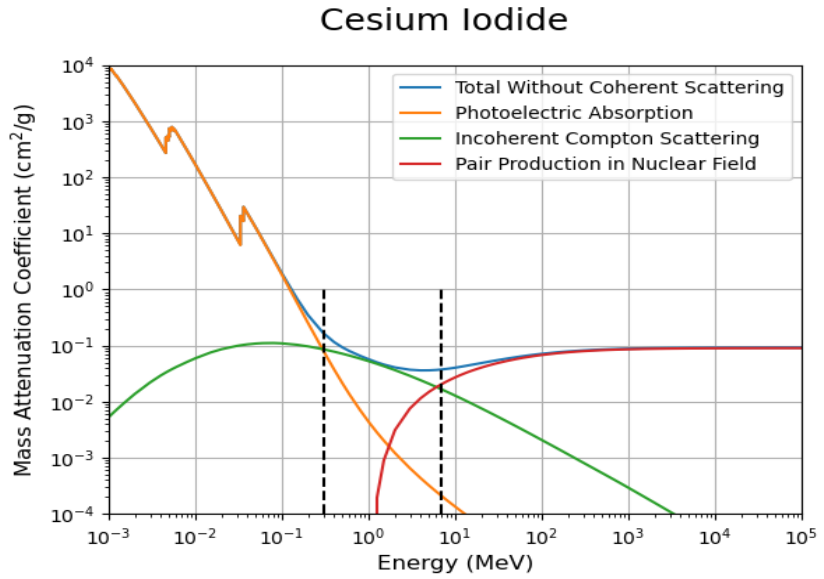

- MeV-GeV detectors need both Compton scattering and pair production measurements
- For low-Z materials, Compton scattering is dominant in the range 50 keV – 15 MeV
- For high-Z materials, such as CsI, Compton scattering only is dominant from ~300 keV to 7 MeV
- Multiple-Compton scattering might happen in the common gamma-ray detector materials

https://physics.nist.gov/PhysRefData/Xcom/html/xcom1.html

Fermi-LAT point spread function (PSF)

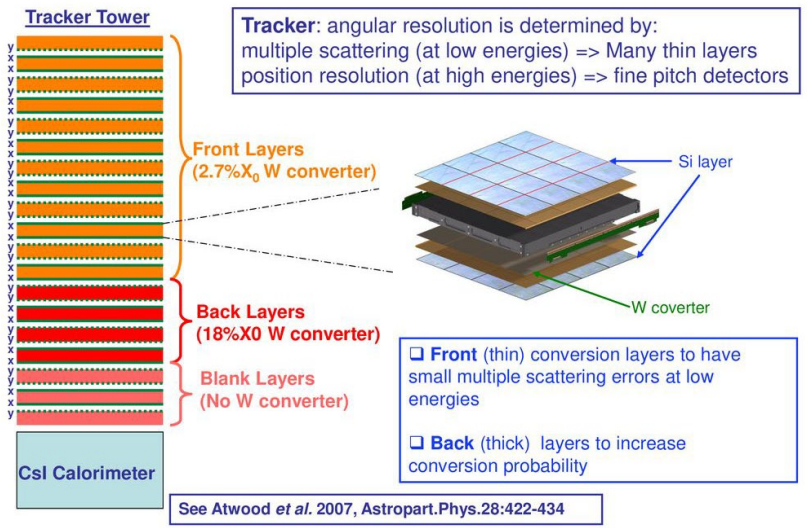

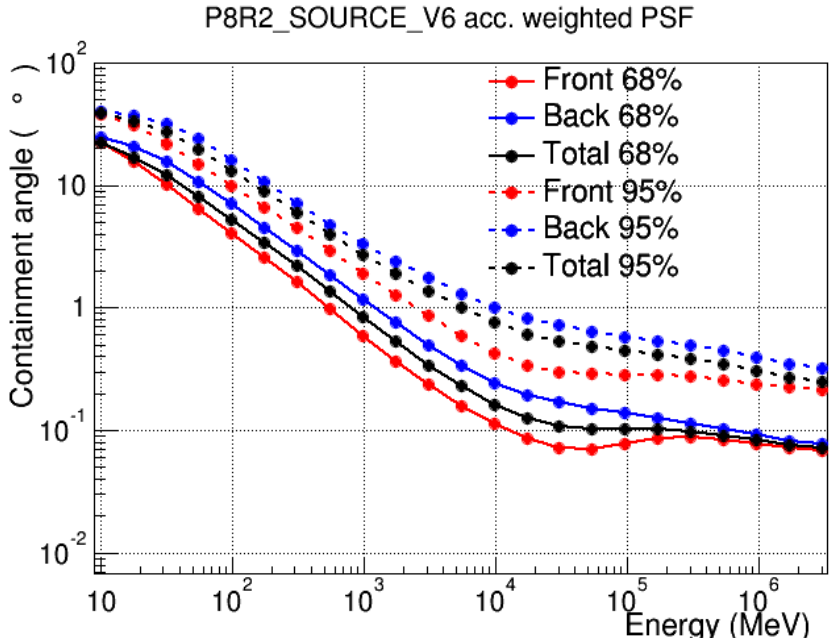

- At low energies the PSF is poor because of multiple scattering of the e^+e^- pairs in the TKR planes with W layers
  - Need to reduce material budget
- At high energies the PSF is limited by the silicon strip pitch (228 µm)

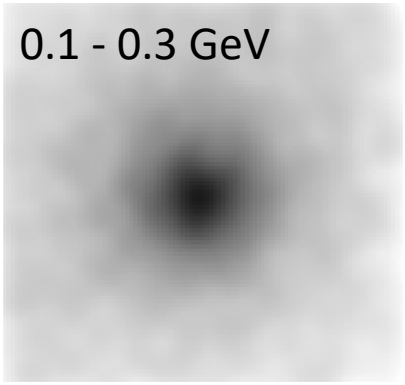

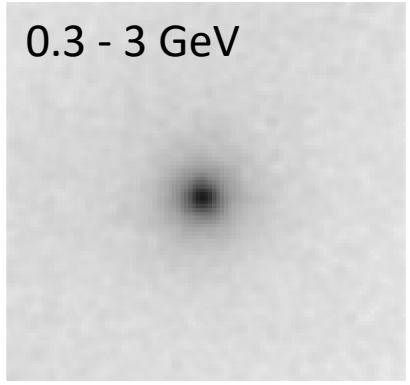

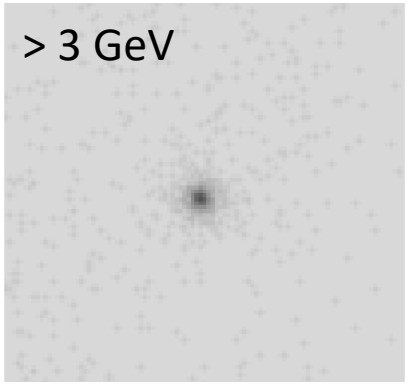

Vela pulsar count maps
(10°×10°, 75 days of data)

Fermi-LAT effective area and acceptance

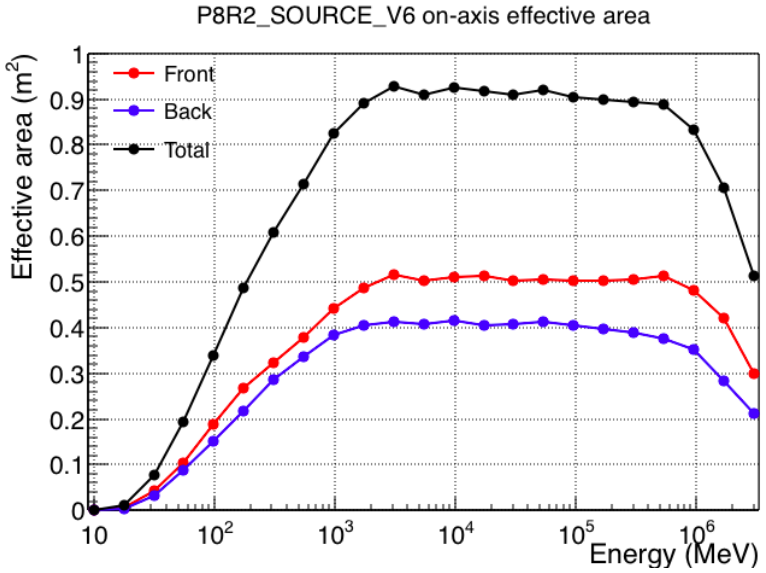

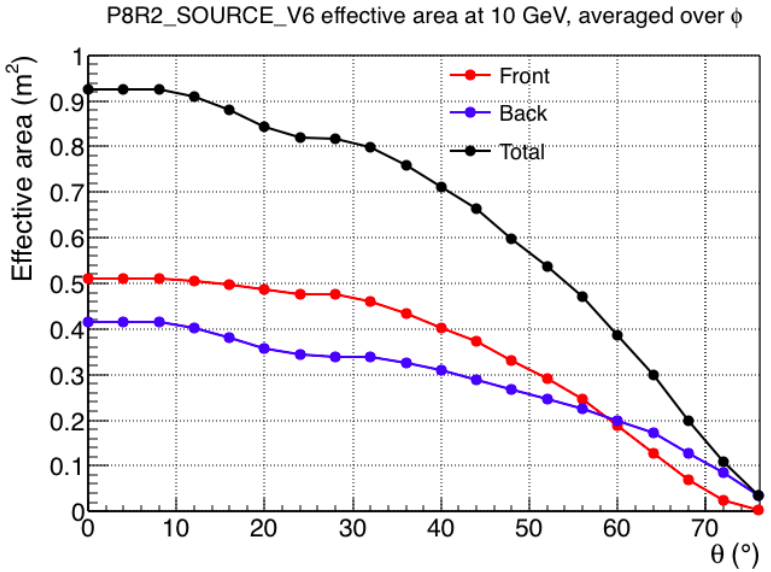

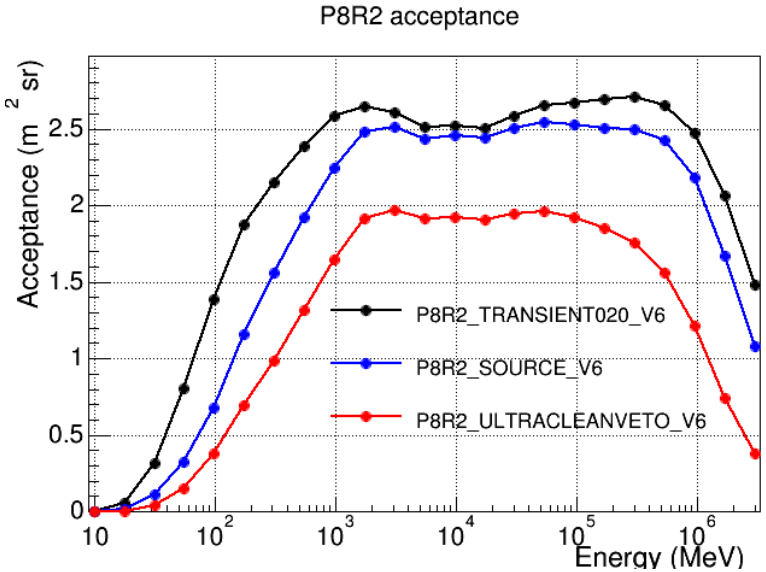

- Drop at E<100 MeV due to the pair production cross section and to the trigger condition, which requires 3 tracker planes in a row
  - Trade-off between gamma-ray conversion and trigger efficiency
- Drop at E>500 GeV due to backsplash in the ACD due to the scintillator tile size

Fermi LAT point-like source sensitivity

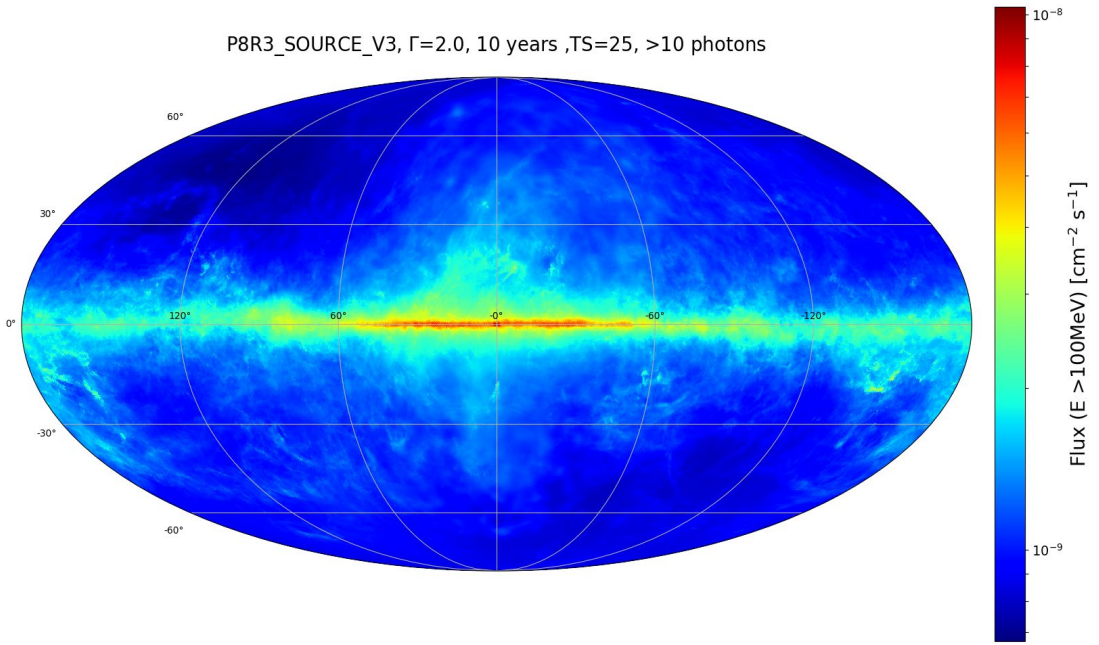

All-sky 10-year integral flux sensitivity for an isolated point source, assuming a power-law spectrum with index 2

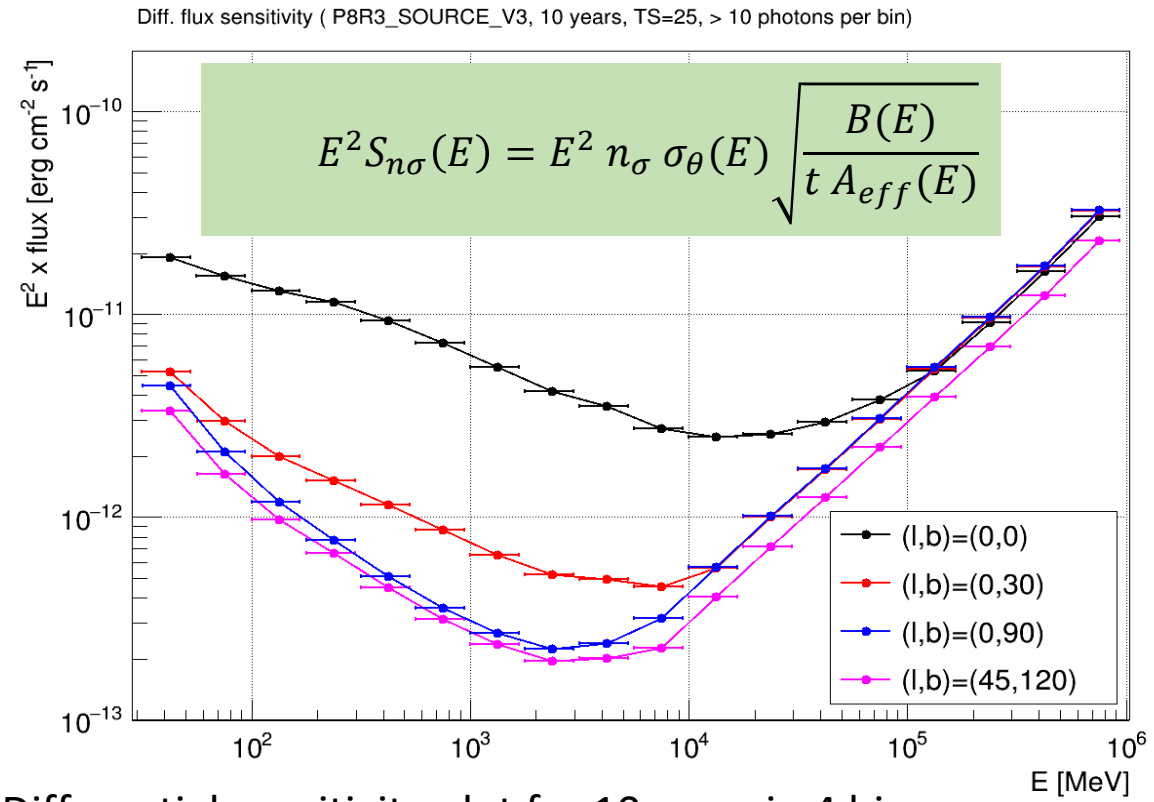

Differential sensitivity plot for 10 years in 4 bins per energy decade between 31.6 MeV and 1 TeV.
It assumes a point source with a power-law spectrum with index 2 and uniform background around it.

https://www.slac.stanford.edu/exp/glast/groups/canda/lat_Performance.htm

COMPTEL telescope

- The imaging Compton telescope COMPTEL is one of the four instruments on board the Compton Gamma-Ray Observatory (CGRO), which was launched in 1991
- COMPTEL consists of two detector arrays
  - upper detector (D1): low-Z material (liquid scintillator NE 213A)
  - lower detector (D2): high-Z material (NaI(Tl) scintillator)
- A gamma ray entering in D1 is Compton-scattered; then the scattered gamma ray makes a second interaction in D2
  - the sequence is confirmed by a time-of-flight measurement
- The locations and energy losses of both interactions are measured

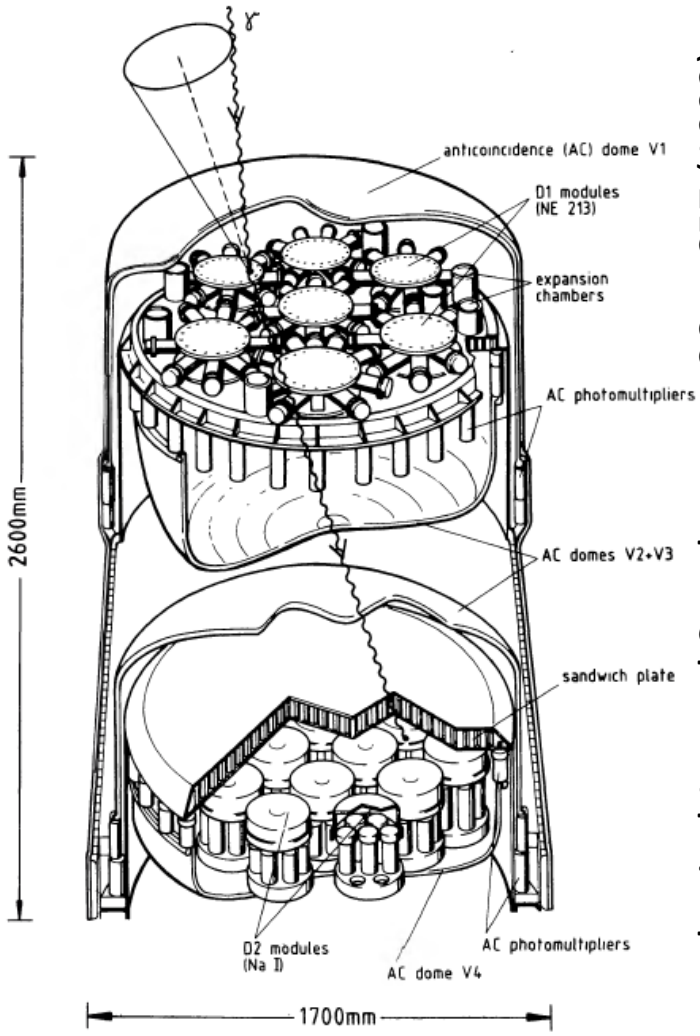

FIG. 2.—Schematic view of COMPTEL

Astrophysical Journal Supplement v.86, p.657 (1993)

Compton telescope (1)

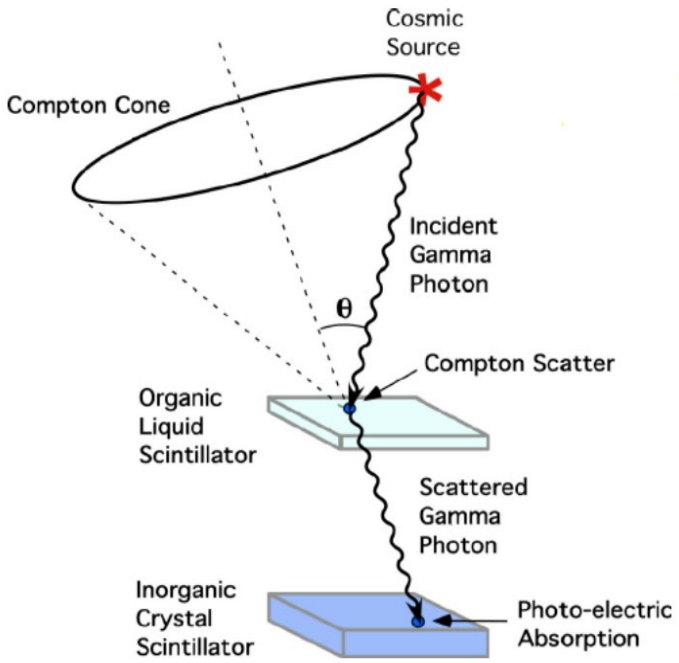

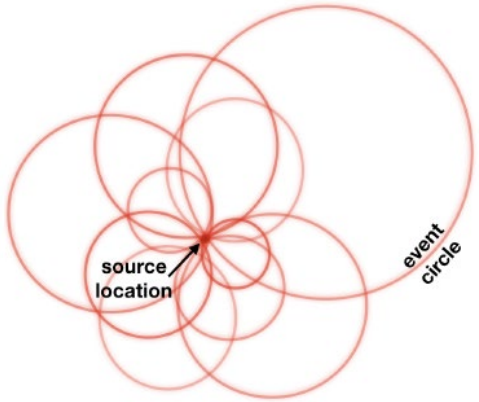

- For completely absorbed events the arrival direction of the gamma-ray is known to lie on the edge of a cone, whose axis is the direction of the scattered gamma ray:

$$\cos\theta = 1 + \frac{m_e}{E_\gamma} - \frac{m_e}{E_\gamma - E_e} = 1 + \frac{m_e}{E_1 + E_2} - \frac{m_e}{E_2}$$

  - θ is the angle between the arrival direction and the direction of the scattered photon; E1 (=Ee) and E2 (=E'γ) are the measured energy losses in first and second interactions
- A celestial source can be therefore located from the circles of different gamma rays from the source
  - Incompletely absorbed events produce circles which do not cross the source position

Compton telescope (2)

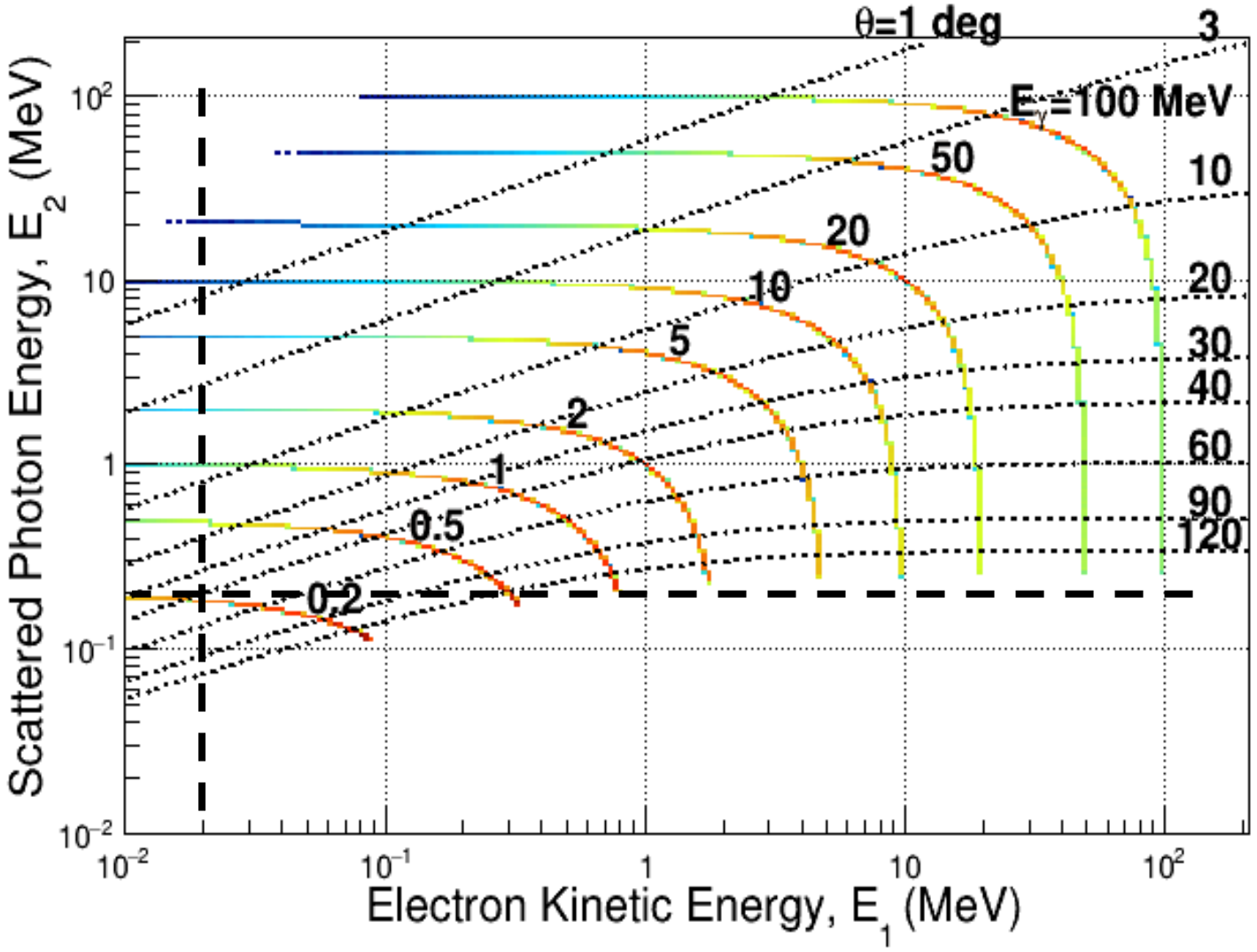

- The hardware energy thresholds of E_1 and E_2 have a significant effect on the field of view of the telescope and on the energy range
- The E_1 threshold defines the lower limit, and the E_2 threshold the upper limit of accepted scattering angles

Next generation gamma-ray telescopes (1)

- COMPTEL's double-scattering concept with large separated planes was a limiting factor for the FoV and measurable Compton scattering angles, and thus led to the low efficiency of the instrument
- Additionally, COMPTEL was only able to measure two-site events, i.e., a single Compton scattering in D1 and a photoelectric absorption in D2
- However, depending on the atomic number of the detector material, a photon can scatter multiple times before finally undergoing a photoelectric absorption
- Ideally, one would want to track the photon trajectory by measuring all secondary (and further) interactions after the initial Compton scattering
- Modern Compton telescopes are based on the concept of a 3D position-sensitive detector volume, acting both as scatterer and absorber

COMPTEL field of view

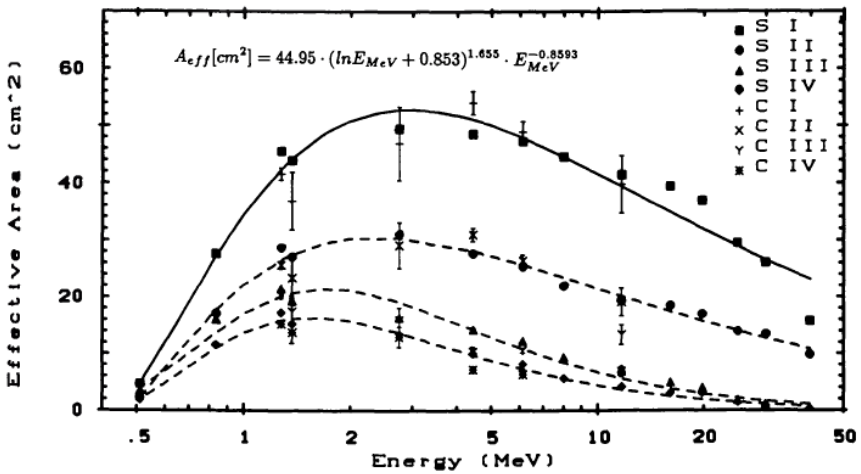

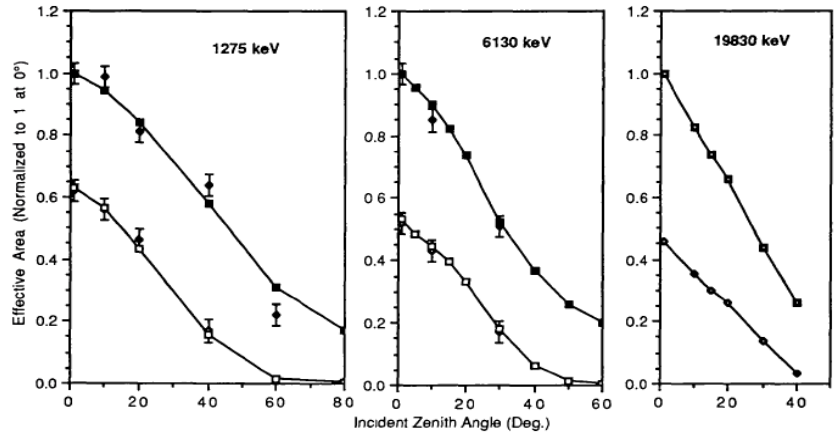

Next generation of gamma-ray telescope (2)

- Combining the scattering and absorbing detector capabilities without large separations allows for the detection of multiple Compton scatterings with no geometric limitation on the scattering angle, as long as the detector volume contains the interactions
  - With modern technological progress, detectors with (sub)mm spatial resolution can be used
  - the efficiency and performance of Compton telescopes have therefore significantly improved in the past few decades since COMPTEL

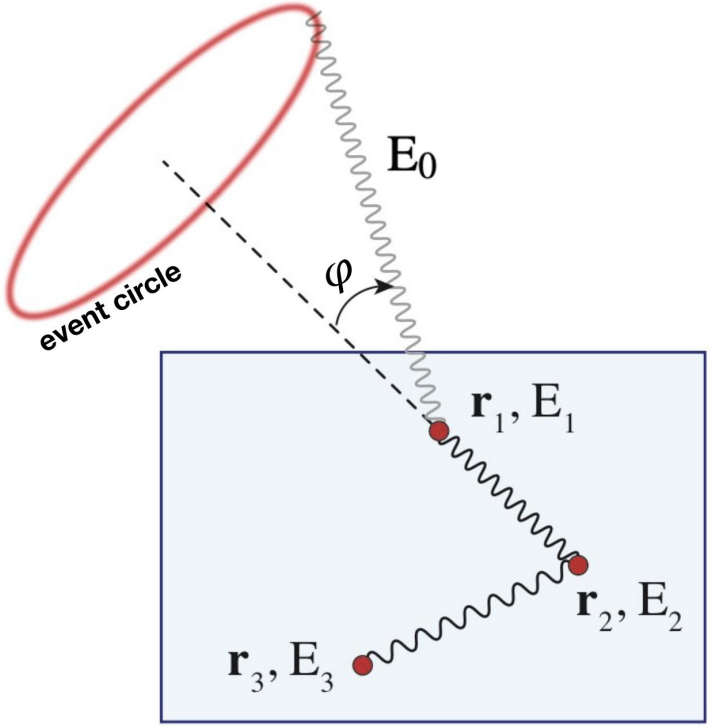

https://arxiv.org/abs/2208.07819

Most modern Compton telescopes use high position-resolution detectors with good energy resolution to measure the position and energy of multiple interactions, with no geometrical limit on the Compton scatter angle

Common configurations for Compton telescopes

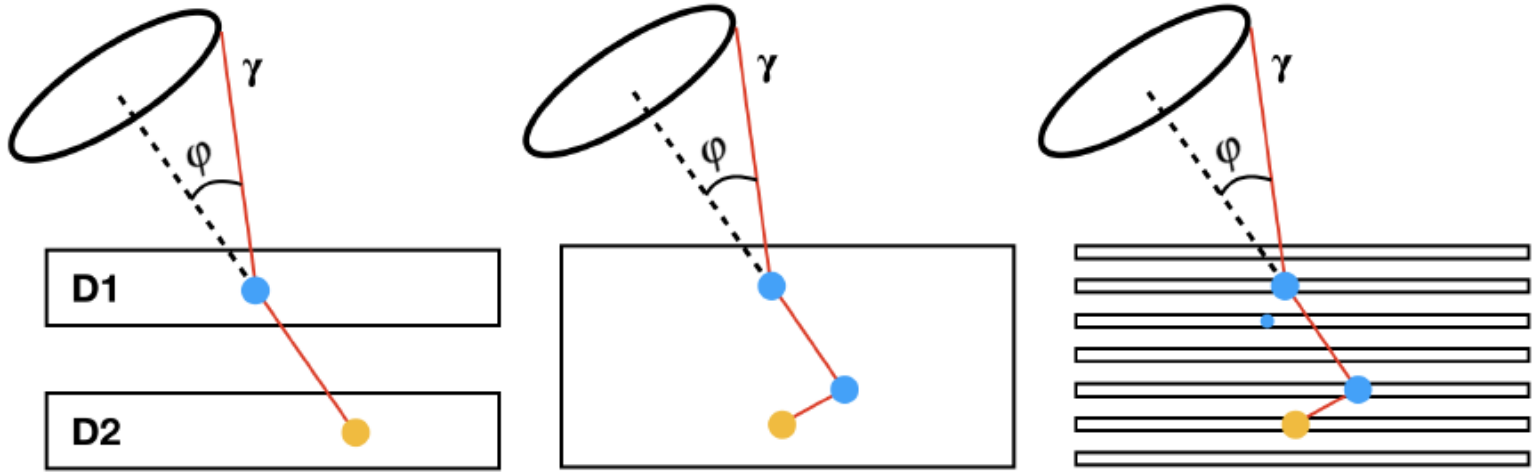

https://arxiv.org/abs/2208.07819

- Left: classic Compton telescope, with two detector planes (scatterer and absorber) to measure double-scattering events
- Middle: compact Compton telescope, with a single 3-D position-sensitive volume (e.g., Time Projection Chamber TPC with liquid gas) to measure multiple Compton scattering events
- Right: multi-layer design , with many thin layers of active detectors (e.g., thin silicon planes), with the possibility of electron tracking

Angular Resolution Measure (ARM)

- The angular resolution of a Compton telescope is given by the width of the Compton Data Space (CDS) cone walls
  - It is generally dominated by the uncertainty in the measured energy and position of interactions

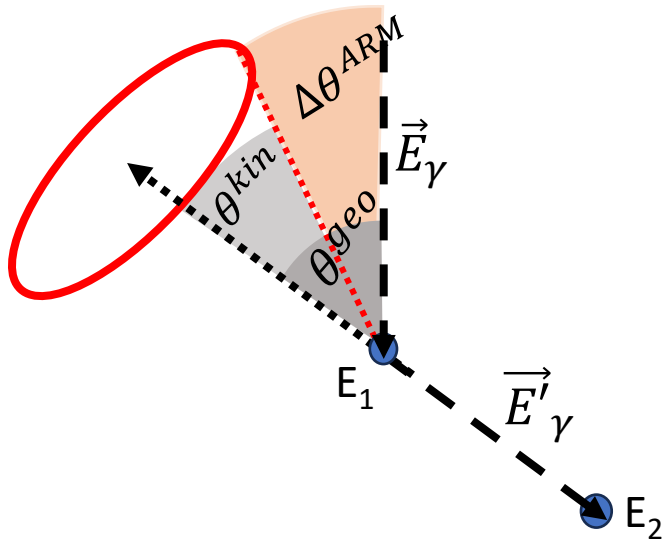

$$\Delta\theta^{ARM} = \theta^{geo} - \theta^{kin}$$

$$\cos\theta^{geo} = \frac{\vec{E}_\gamma \cdot \vec{E'}_\gamma}{|\vec{E}_\gamma|\,|\vec{E'}_\gamma|}$$

$$\cos\theta^{kin} = 1 + \frac{m_e}{E_1 + E_2} - \frac{m_e}{E_2}$$

Uncertainties on the Angular Resolution

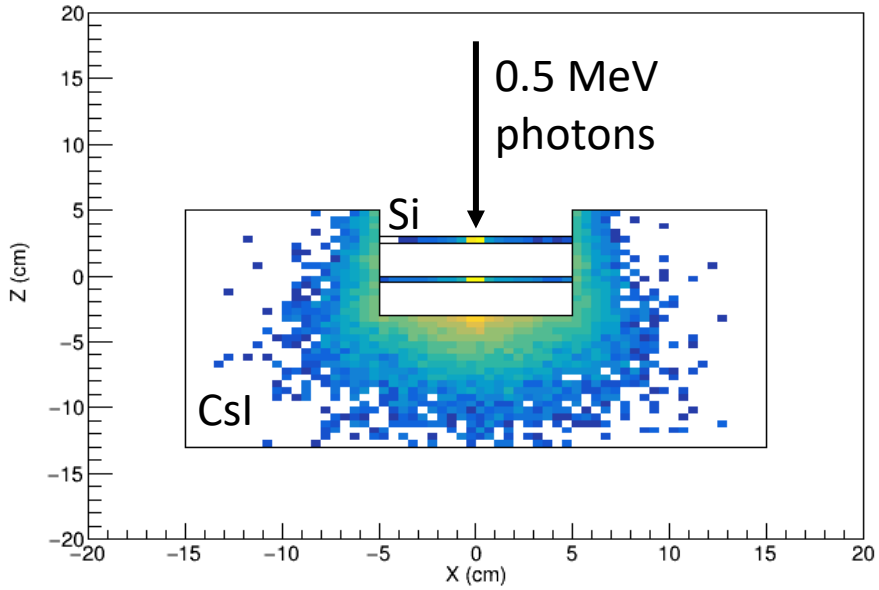

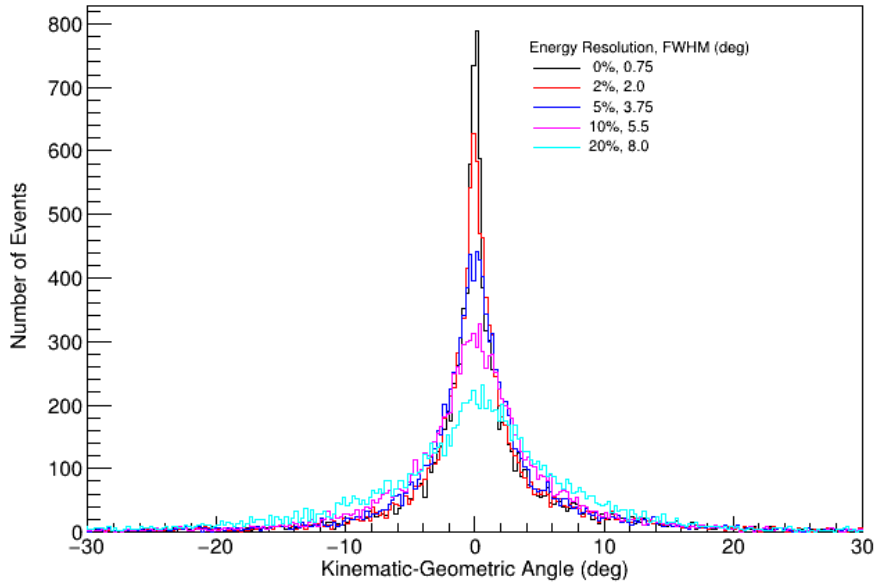

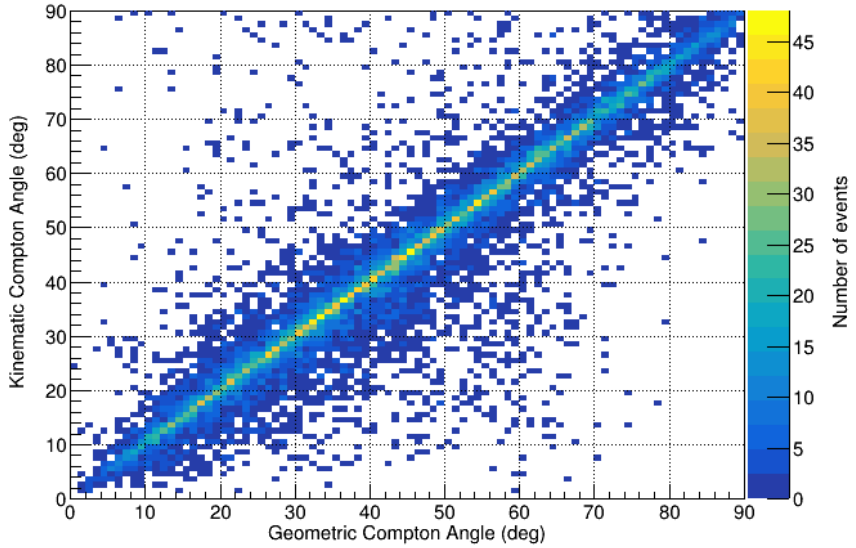

- The angular uncertainty for each event can be determined from the uncertainties in the measured energies, which contribute to the evaluation of the Compton-scattering angle (kinematic angle)
  - The uncertainties on the energy should be kept as low as possible
- The uncertainties in the measured positions due to the finite detector granularity also affects the angular uncertainty

Tracking of Compton electron

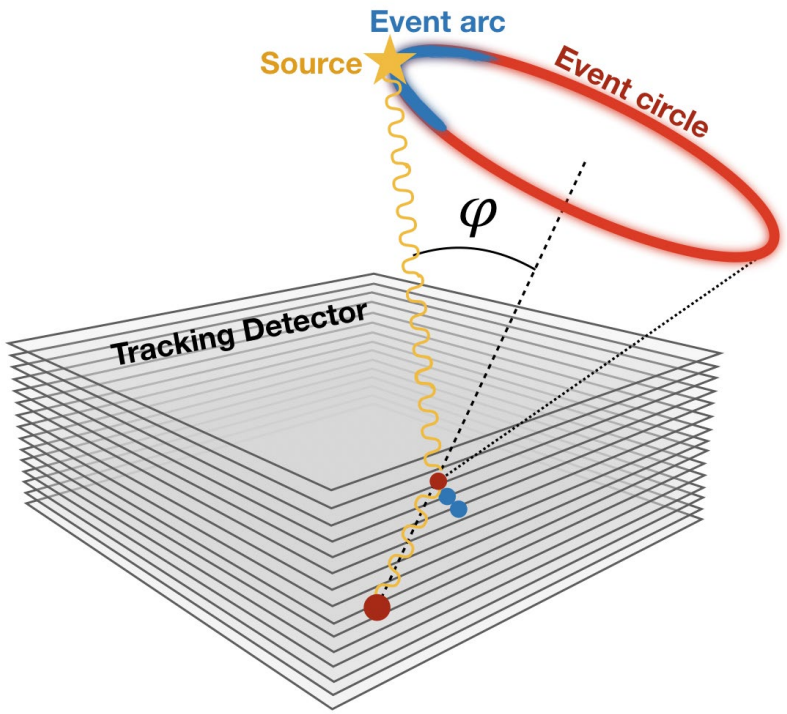

https://arxiv.org/abs/2208.07819

- If the direction of the recoil electron is known, momentum conservation can further restrict the direction of the incident gamma-ray
  - The background rejection can be improved
- By measuring the direction of the Compton-scattered electron in the first interaction, the incident photon direction can be constrained to a reduced arc of the original Compton event circle
  - The length of the event arc depends on the uncertainty in the electron's recoil direction
  - Require excellent 3D-point resolution and energy resolution

Tracked Vs untracked Compton events

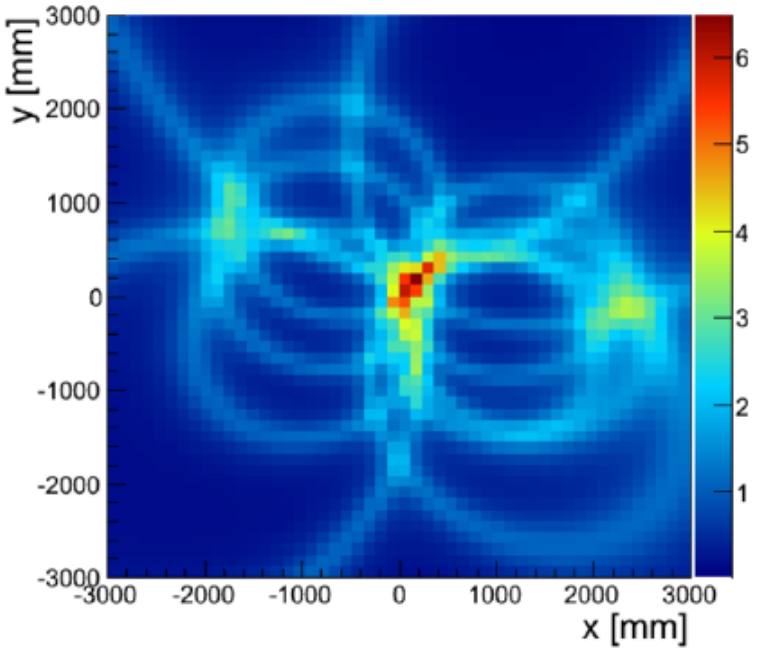

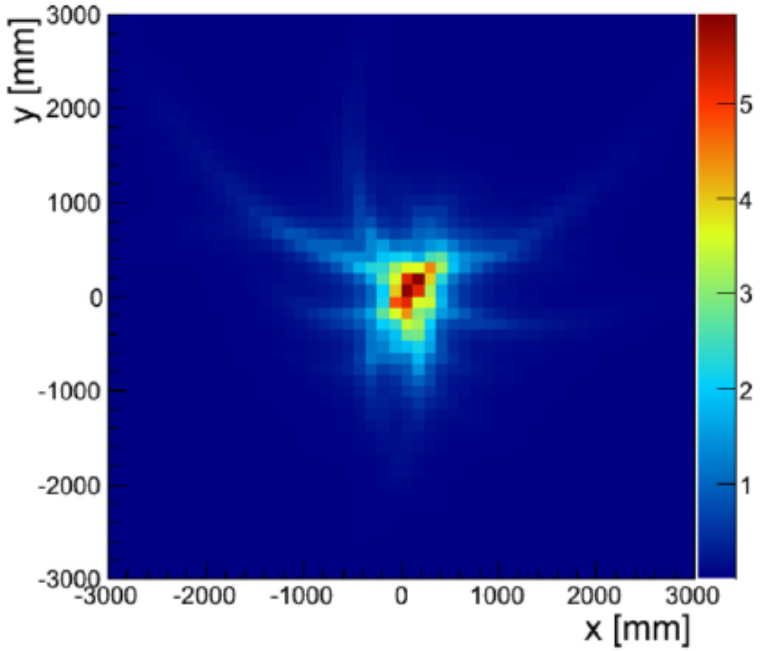

Y Mizumura et al 2014 JINST 9 C05045

- Comparison of imaging of a few gamma rays without “untracked Compton events” (left plot) and with electron tracking “Tracked Compton events” (right plot)
- Electron tracking can enhance the sensitivity of a telescope since the background contamination can be significantly reduced

ESA M-call proposals: ASTROGAM projects

- eASTROGAM M5-Esa call (2016-2018) – Low Earth Orbit (LEO)
  - Tracker: nearly 56 m2 of double-sided Si strip detectors (DSSDs)
  - 4 towers, 56 layers of 5×5 DSSDs (5600 wafers, 9.5 cm wide, 500 µm thick and 240 µm of pitch)
  - Calorimeter: CsI fingers (LxWxH) 0.5x0.5x8 cm^3 read-out with silicon drift detector (SDD)
  - Exper. Astron. 44 (2017) 1, 25-82
- ASTROGAM M7-Esa call (2021-2022) – LEO
  - Tracker: 4 towers, 30 x 30 cm2 cross section, with 65 layers of 500 µm silicon thick wafers
    - Baseline: 3x3 arrays of 10 cm side DSSD
    - Option: Silicon pixel detectors
  - Calorimeter: 56 x 56 CsI finger bars of (LxWxH) 1x1x8 cm^3 read-out with SDD (option SiPM)

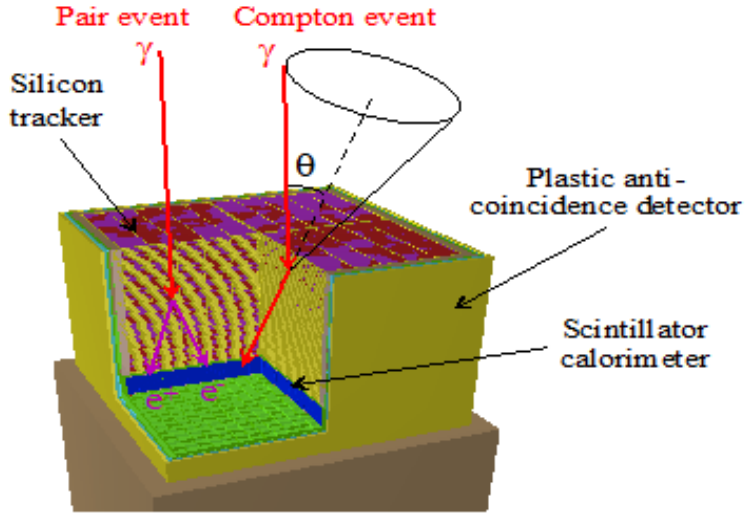

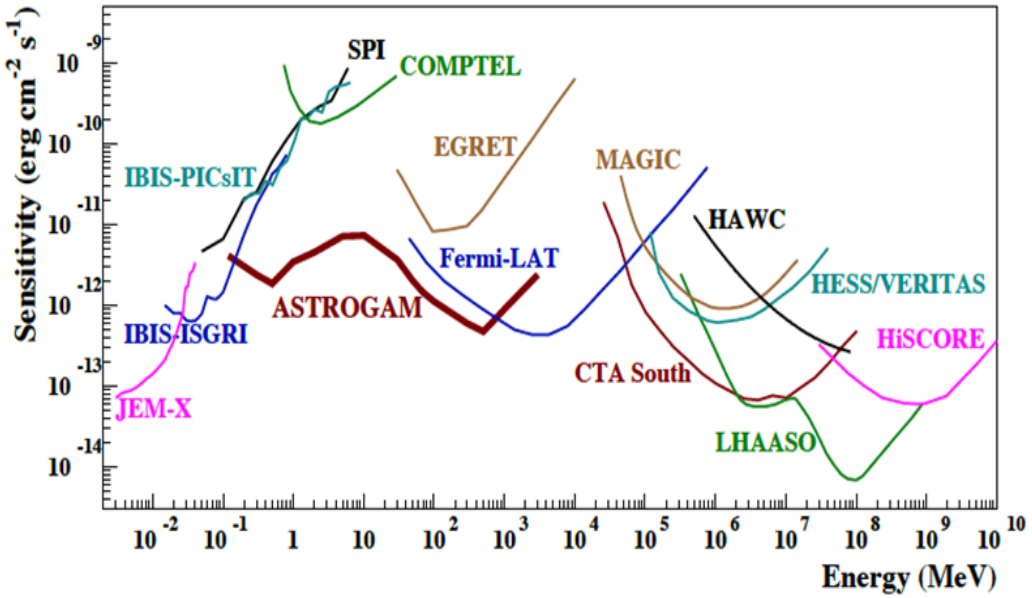

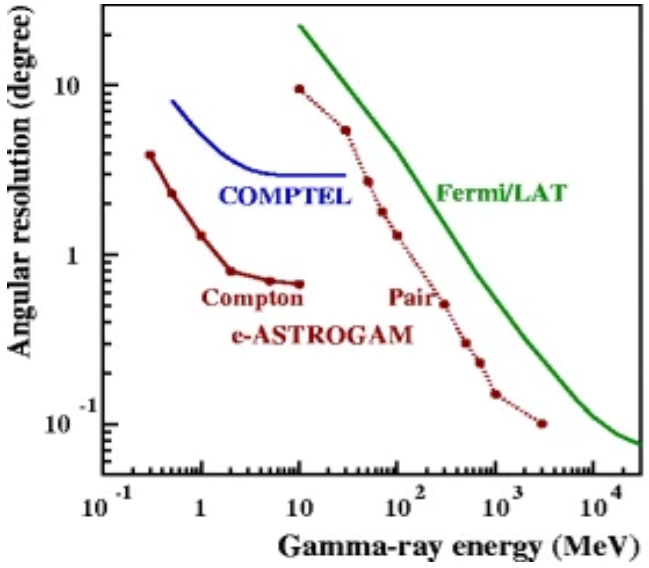

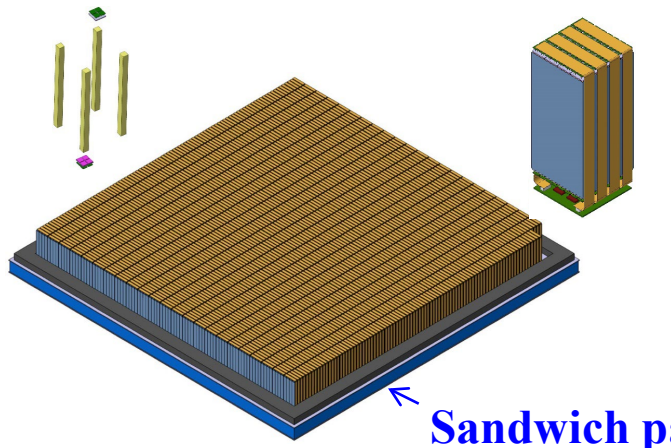

AMEGO-X proposal to MIDEX

- AMEGO-X proposal submitted to the Midex (2021):
  - Reduced-scale version of the AMEGO instrument as probe mission
- Silicon tracker: large pixel size (500 x 500 μm^2), 500 μm thick – Monolithic CMOS pixel
  - Option: double-sided silicon strip detector
- Hodoscopic calorimeter: CsI crystal bars
- Anticoincidence system: based on plastic scintillator tiles
- For further details: https://arxiv.org/abs/2208.04990

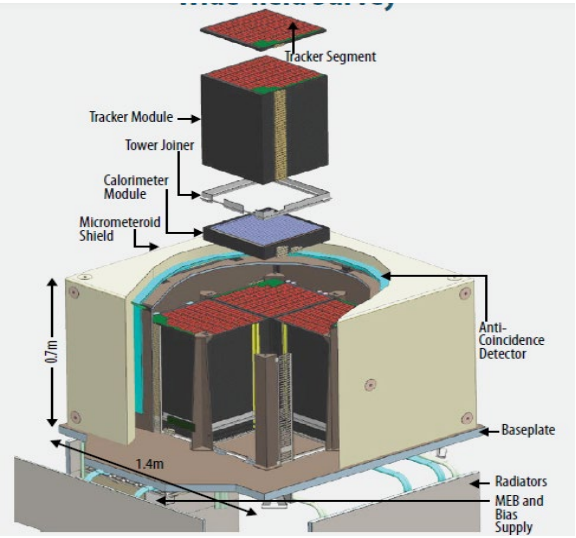

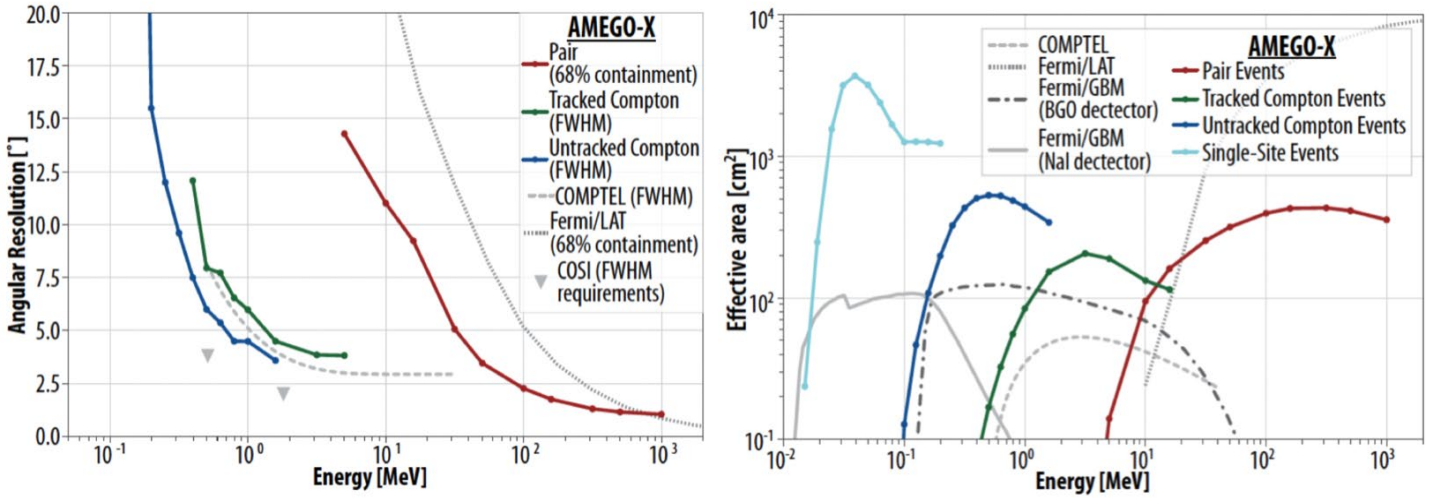

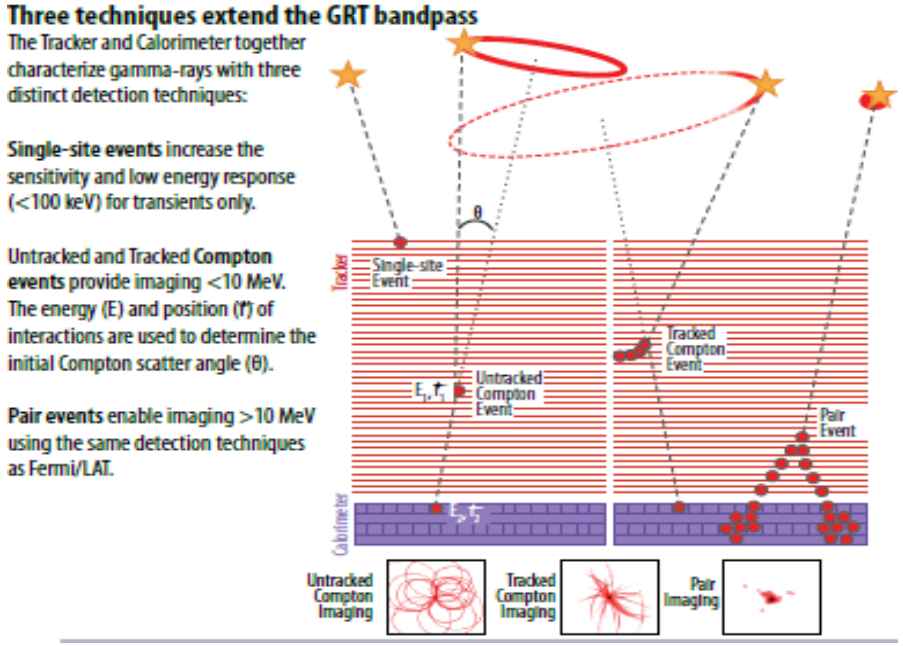

The Advanced Particle-astrophysics Telescope (APT)

- The APT detector design (3m x 3m x 2.5m):
  - mission concept for a space-based gamma-ray and cosmic-ray explorer
    - Combine a pair and Compton telescope in one design (like AMEGO, ASTROGAM).
  - 20 layers of 5mm thick CsI(Na) with crossed wavelength shifting fiber (WLS fiber) readout
  - 20 x - y scintillating optical fiber tracker (SOFT) layers using interleaved 1.5mm round scintillating fibers
  - With the addition of foam radiators, the CsI detectors could detect the transition radiation X-rays from very-high-energy light cosmic rays
  - Top-bottom symmetry doubles FoV (in L2 orbit)
  - Read out on the sides with SiPM photodetectors and analog-pipeline waveform digitizers
- A recent NASA grant to develop a full suborbital mission, the Advanced Demonstrator for APT (ADAPT), targeting a long-duration flight on a 60 million-cubic-foot balloon flight from Antarctica in the FY25 season
  - For more details see Di Venere's talk

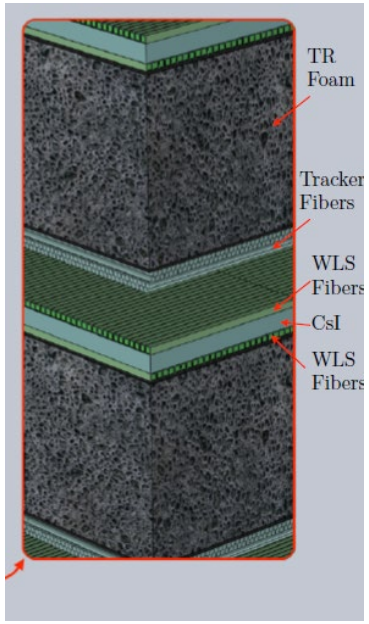

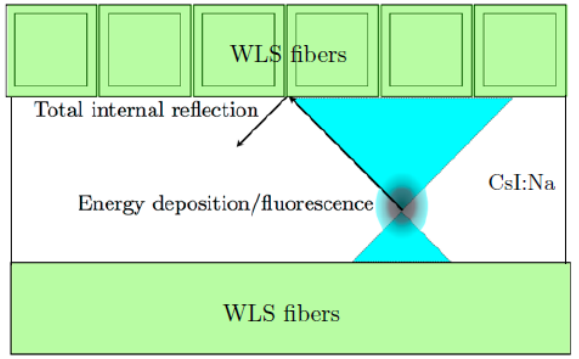

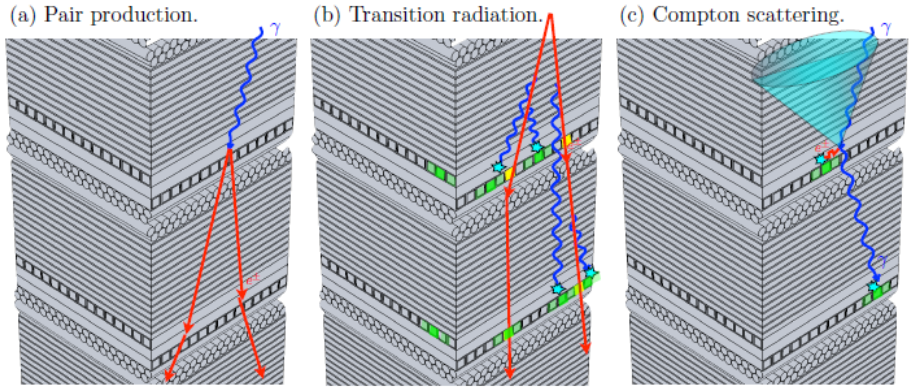

CRYSTAL EYE proposal

- Combining single-hit and 2-point layout
- Sphere layout
  - Radius: ~20 cm
  - Mass: <50 kg
  - Energy range: 10 keV – 30 MeV
  - Material: LYSO
  - Photodetectors: SiPM-array
  - FOV: 2π
- COMPACT SIZE:
  - Free-flyer
  - Onboard of space stations
  - GBM module of larger satellites
- For more details see
  - Felicia Barbato's talk
  - Roberta Colalillo's poster

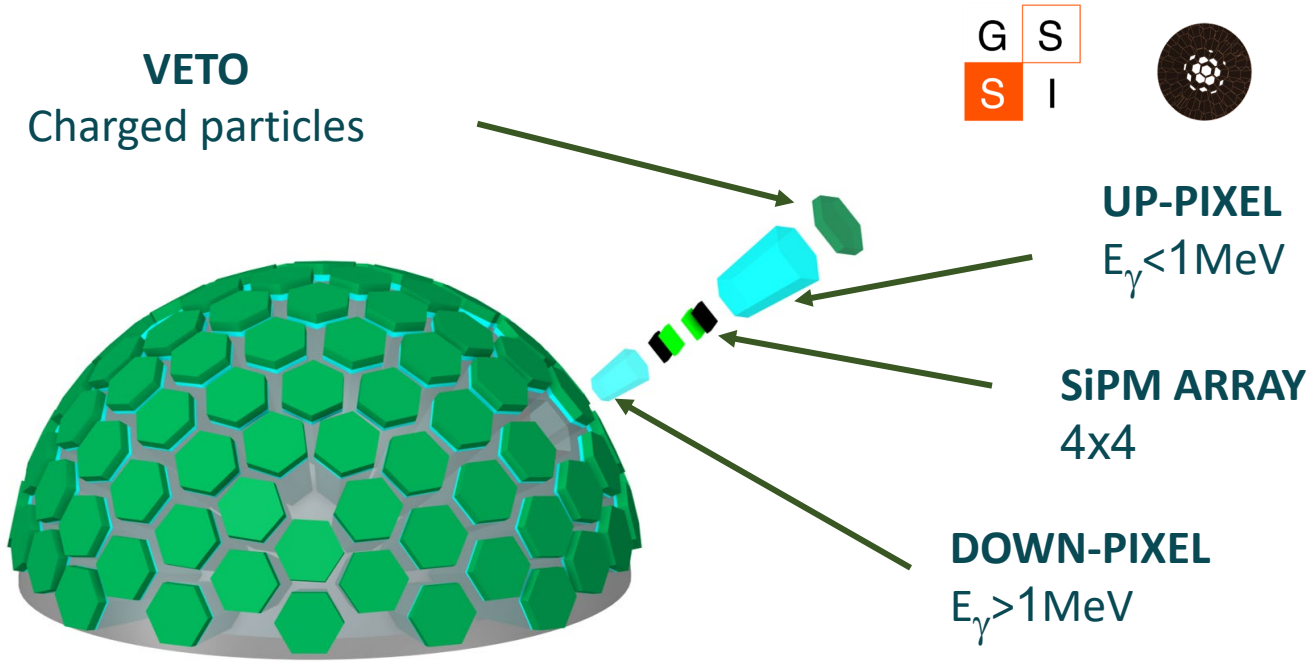

Conclusions

- Fermi-LAT observations at MeV-GeV energies have opened a window to a rich and varied ensemble of astrophysical sources
  - An equally rich return from opening the MeV-GeV band is expected
- We are at the dawn of the multi-messenger era, with the recent discovery of high energy astrophysical neutrinos by IceCube and the first direct observation of gravitational waves by LIGO
- A medium energy gamma-ray surveyor is an excellent partner in these new scientific endeavors
  - Capability of measuring polarization in the MeV-GeV band

Backup

Point-like source sensitivity (1)

- The point-like source sensitivity of a given instrument depends on the effective area and point spread function of the detector, the observation time toward a given direction in the sky and the intensity of the background emission around the same direction
- The number of signal events (e.g. gamma rays) s detected for a point-like integral source flux S in a given energy range is given by:

$$s = t\, A_{eff}\, S\, \epsilon_{PSF}$$

- If we assume that the background is locally uniform with integral intensity B, the number of background events is:

$$b = t\, A_{eff} B\, \Delta\Omega(\epsilon_{PSF})$$

- Where $\Delta\Omega(\epsilon_{PSF})$is the solid angle corresponding to a given PSF containment, e.g. $\epsilon_{PSF} = 0.90 \implies \Delta\Omega(\epsilon_{PSF}) = 2\pi(1 - \cos\theta_{90\%}) \approx \pi\, \theta_{90\%}^2$

Point-like source sensitivity (2)

- The signal to noise ratio is:

$$\frac{s}{\sqrt{b}} = \frac{t\,A_{eff}\,S\,0.90}{\sqrt{t\,A_{eff} B\pi\,\theta_{90\%}^2}} = S\frac{0.90}{\theta_{90\%}}\sqrt{\frac{t\,A_{eff}}{\pi\,B}}$$

- The signal to noise ratio improves with the square root of exposure ($t\,A_{eff}$= live time times effective area) and linearly with the angular resolution
- The minimum signal flux above a given number of sigma nσ (e.g., 5) above the noise $S_{n\sigma}$ is given by:

$$S_{n\sigma} = n_\sigma\,\frac{\theta_{90\%}}{0.90}\sqrt{\frac{\pi B}{t\,A_{eff}}}$$

Compton telescope (2)

- As detectors are sensitive to the ionization from the recoil electron, it is important to consider the kinetic energy of the Compton-scattered electron (ERS system):

$$E_e = E_\gamma - E_\gamma{}' = E_\gamma - \frac{E_\gamma}{1 + \frac{E_\gamma}{m_e}(1 - \cos\theta)} = E_\gamma \frac{E_\gamma(1 - \cos\theta)}{m_e + E_\gamma(1 - \cos\theta)}$$

- For head-on collision θ=180° the maximum amount of energy is transferred to the electron

$$E_e^{max}|_{\theta=180^\circ} = E_\gamma \frac{2E_\gamma}{m_e + 2E_\gamma} = E_\gamma \left(1 - \frac{1}{1 + \frac{2E_\gamma}{m_e}}\right)$$

- The difference between the initial photon energy and the maximum recoil electron energy is given by

$$E_c = E_\gamma - E_e^{max}|_{\theta=180^\circ} = \frac{E_\gamma}{1 + \frac{2E_\gamma}{m_e}}$$

Compton telescope (3)

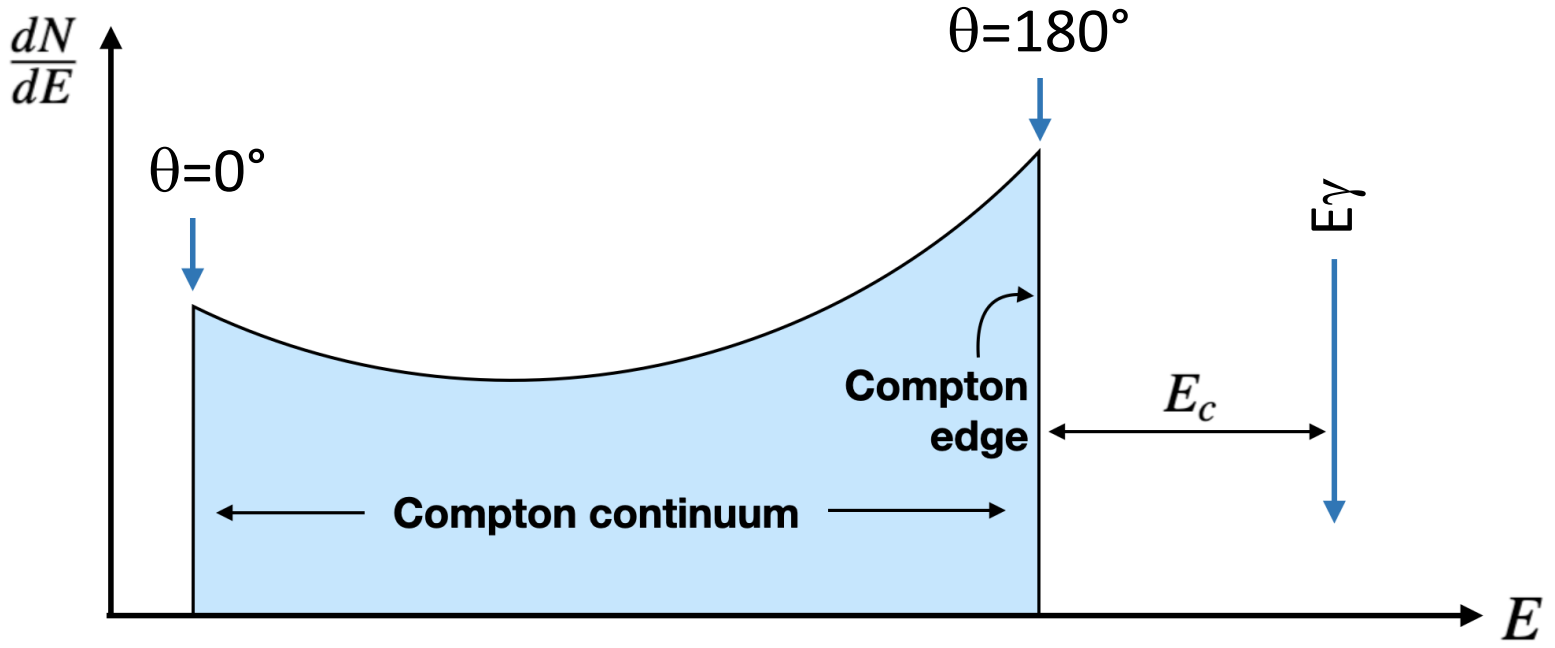

- The spectral shape of the recoil electron energy for a photon with initial energy Eγ
- There is a continuum of electron energies observed due to the range of allowable Compton scatter angles
- The maximum recoil electron energy is achieved for backscatter interactions when θ=180°: this defines what is referred to as the Compton edge in a measured spectrum

ASTROGAM M7 proposal

- Tracker:
  - 4 towers, 30 x 30 cm^2 cross section, with 65 layers of 500 μm silicon thick wafers
  - Baseline: 3x3 arrays of 10 cm side double-sided square silicon strip detectors
  - Option: Silicon pixel detectors
- Calorimeter:
  - 56 x 56 CsI finger bars of (LxWxH) 1x1x8 cm^3
- Anticoincidence system:
  - plastic scintillators read-out by SiPMs
- Equatorial low-Earth orbit
  - Inclination i < 2.5°
  - Eccentricity e < 0.01
  - altitude 550 – 600 km
- Fits with the Vega-C launcher

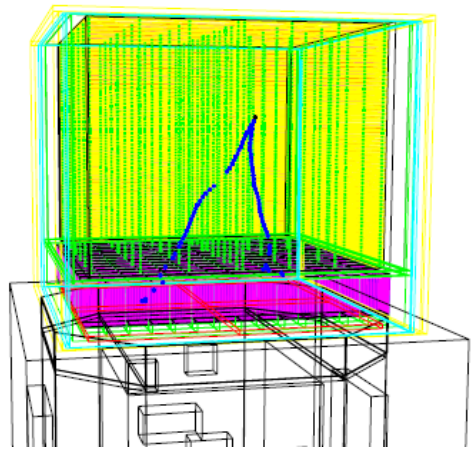

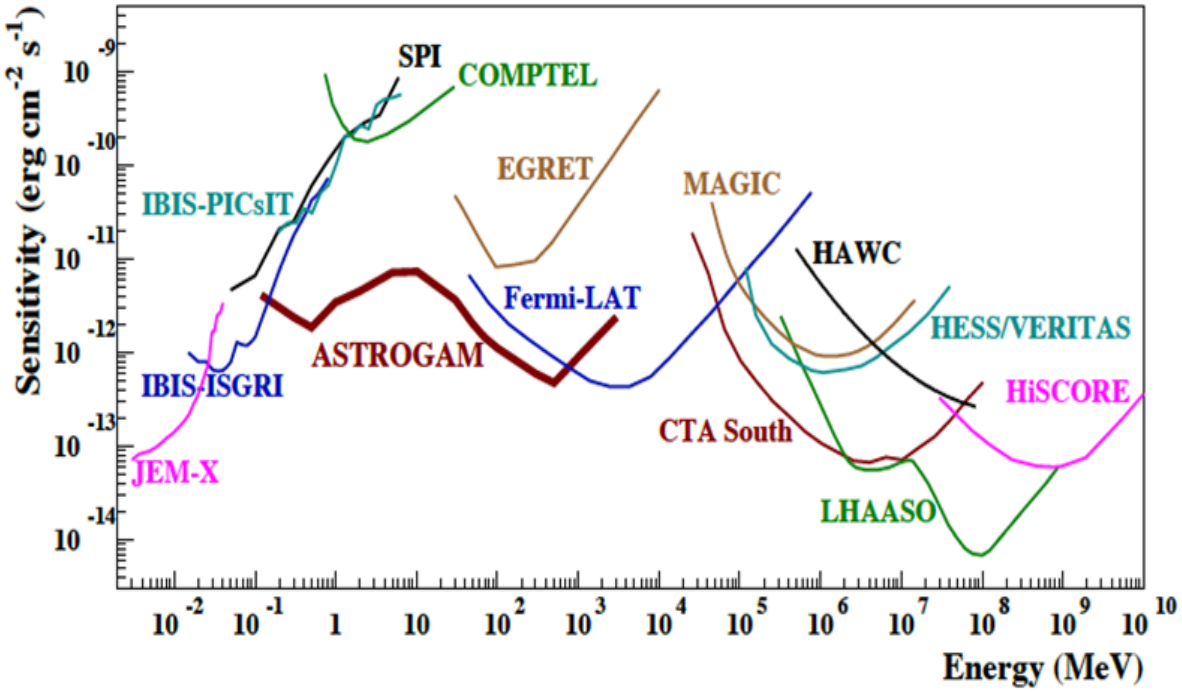

At the heart of the extreme Universe

- How does the accretion disk/jet transition occur around supermassive black holes in AGN?
- Are BL Lacs sources of UHECRs and high-energy neutrinos?
- Launch of ultra-relativistic jets in GRBs? Ejecta composition, radiation processes?
- Can short-duration GRBs be unequivocally associated to gravitational wave signals?
- With a wide field of view, unprecedented sensitivity over a large spectral band, and exceptional capacity for polarimetry, MeV-GeV telescope will give access to a variety of extreme transient phenomena

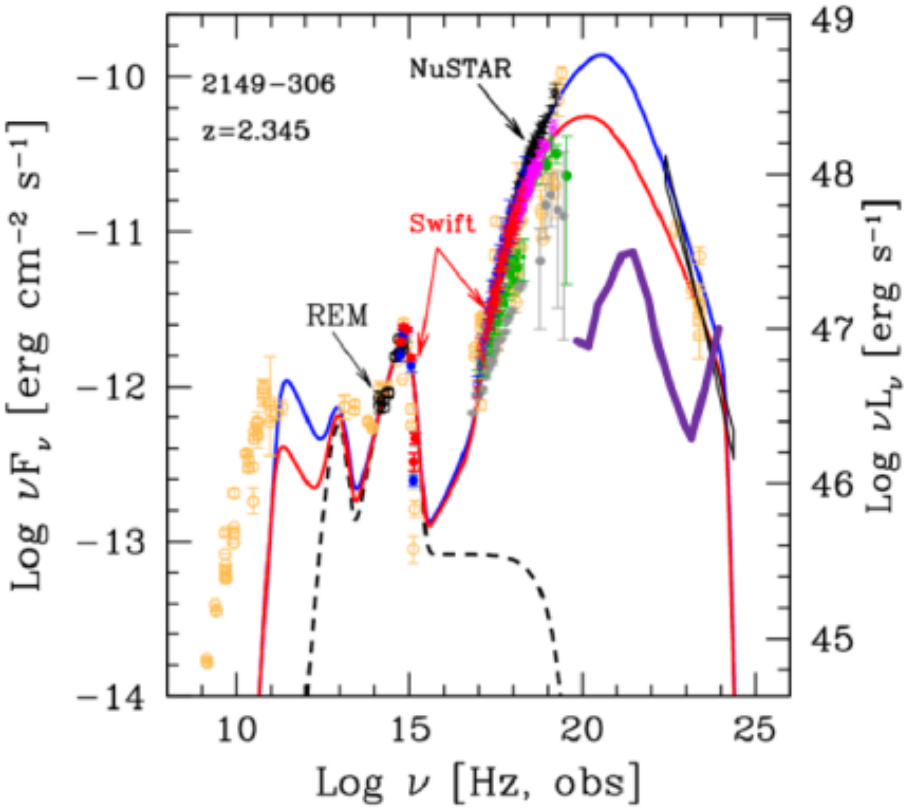

TXS 0506+056

- Relativistic jets produce gamma rays through the interactions of the particles they accelerate
  - In leptonic models, accelerated electrons produce all observed gamma rays, principally via synchrotron and inverse Compton emission
  - In hadronic models, accelerated protons produce gamma rays through proton-synchrotron radiation or via synchrotron radiation from secondary particles generated by proton interactions with jet photons (via e.g., photo-pion production), the latter of which also produces neutrinos
  - For most flare data from currently operating observatories, it is not possible to determine which scenario better describes the data – both hadronic and leptonic models are consistent with observed blazar spectra
- The brightest neutrino events may not be detected by higher-energy gamma-ray telescopes, such as the Fermi/LAT, because the radiation fields required for efficient neutrino production make the source opaque to high-energy gamma rays
  - Need to monitor the sky in the MeV band

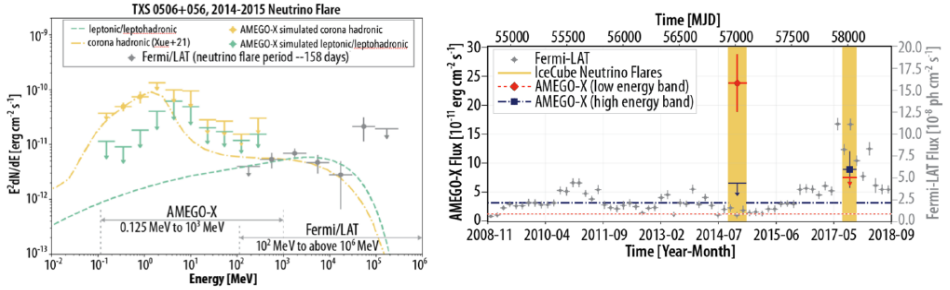

Fig 1: Simulated AMEGO-X SED for the 2014 flare of TXS 0506+056. The green dashed line is representative of leptonic and leptohadronic models, while the yellow dot-dashed line is the two-zone hadronic model where one of the zones is from the AGN corona from Ref.[23] The gray data points are measurements from Fermi/LAT (left). Light-curve of TXS 0506+056. The gray data points are measurements from Fermi/LAT. The yellow band show the times of the IceCube neutrino flares (right). The green data points are simulated AMEGO-X detection of the MeV emission during those flares. See[18] for more details.

Supernovae, nucleosynthesis, and Galactic chemical evolution

- How do thermonuclear and core-collapse SNe explode? How are cosmic isotopes created in stars and distributed in the interstellar medium?
- With a remarkable improvement in gamma-ray line sensitivity over previous missions, a new MeV-GeV telescope should allow us to finally understand the progenitor system(s) and explosion mechanism(s) of Type Ia SNe (56Ni, 56Co), the dynamics of core collapse in massive star explosions (56Co, 57Co), and the history of recent SNe in the Milky Way (44Ti, 60Fe...)

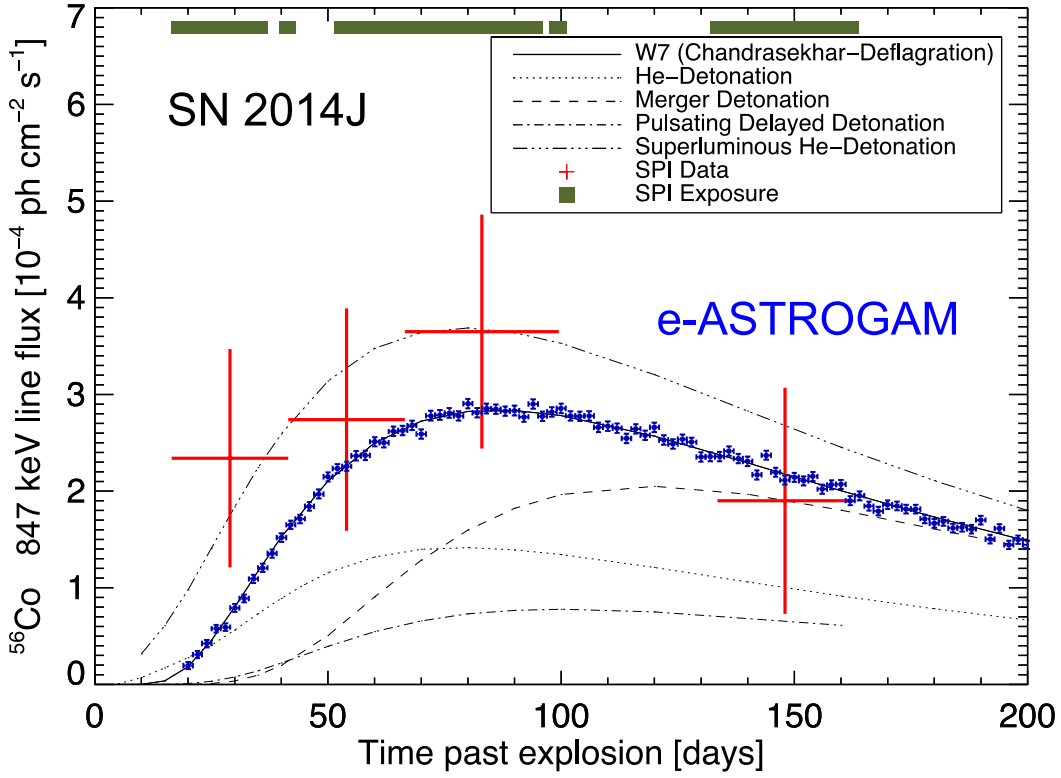

Supernova remnants, Novae and Star-formation Regions

- The smoking gun to identify accelerators of CR protons is to detect the characteristic neutral pion decay ($\pi_0 \rightarrow 2\gamma$) feature, or pion bump, produced in the interaction of protons with the interstellar material.
  - Each photon produced has an energy of 67.5 MeV (in the π_0 rest frame) which is ideally matched to the ASTROGAM/AMEGO band
- Proton acceleration is thought to happen in supernova remnants (SNRs), novae, and star-forming regions (SFRs)

https://arxiv.org/abs/2208.04990